Title
Development of an Adaptive Corridor Traffic Control Model

Authors
Recker, Will
Zhenhg, Xing
Chu, Lianyu

Publication Date
2010-03-01

CALIFORNIA PATH PROGRAM
INSTITUTE OF TRANSPORTATION STUDIES
UNIVERSITY OF CALIFORNIA, BERKELEY

Development of an Adaptive Corridor Traffic Control Model

Will Recker, Xing Zheng, Lianyu Chu

California PATH Research Report
UCB-ITS-PRR-2010-13

This work was performed as part of the California PATH Program of the University of California, in cooperation with the State of California Business, Transportation, and Housing Agency, Department of Transportation, and the United States Department of Transportation, Federal Highway Administration.

Final Report for Task Order 6323

March 2010

ISSN 1055-1425

FINAL REPORT

Caltrans RTA 65A0208 (PATH T.O. 6323)

Optimal Control for Corridor Networks: A Mathematical Modeling Approach

Prepared by:

Will Recker, Xing Zheng

Institute of Transportation Studies
University of California, Irvine
Irvine, CA 92697

Lianyu Chu
California Center for Innovative Transportation
University of California, Berkeley
Berkeley, CA 94720

November, 2009

STATE OF CALIFORNIA DEPARTMENT OF TRANSPORTATION

TECHNICAL REPORT DOCUMENTATION PAGE

TR0003 (REV. 10/98)

1. REPORT NUMBER	2. GOVERNMENT ASSOCIATION NUMBER	3. RECIPIENT'S CATALOG NUMBER
CA10-0759		

4. TITLE AND SUBTITLE	5. REPORT DATE
Optimal Control for Corridor Networks: A Mathematical Modeling Approach	November 2009 6. PERFORMING ORGANIZATION CODE

7. AUTHOR(S)	8. PERFORMING ORGANIZATION REPORT NO.
Will Recker, Lianyu Chu, Xing Zheng	UCB-ITS-PRR-2010-13

9. PERFORMING ORGANIZATION NAME AND ADDRESS	10. WORK UNIT NUMBER
Institute of Transportation Studies University of California, Irvine Irvine, CA 92697-3600	193 11. CONTRACT OR GRANT NUMBER 65A0208

12. SPONSORING AGENCY AND ADDRESS	13. TYPE OF REPORT AND PERIOD COVERED
California Department of Transportation Division of Research and Innovation, MS-83 1227 O Street; Sacramento CA 95814	Final Report 14. SPONSORING AGENCY CODE

15. SUPPLEMENTAL NOTES

None

16. ABSTRACT

This research develops and tests, via microscopic simulation, a real-time adaptive control system for corridor management in the form of three real-time adaptive control strategies: intersection control, ramp control and an integrated control that combines both intersection and ramp control. The development of these strategies is based on a mathematical representation that describes the behavior of traffic flow in corridor networks and actuated controller operation. Only those parameters commonly found in modern actuated controllers (e.g., Type 170 and 2070 controllers) are considered in the formulation of the optimal control problem. As a result, the proposed strategies easily could be implemented with minimal adaptation of existing field devices and the software that controls their operation. Microscopic simulation was employed to test and evaluate the performance of the proposed strategies in a calibrated network. Simulation results indicate that the proposed strategies are able to increase overall system performance and also the local performance on ramps and intersections. Prior to testing the complete model, separate tests were conducted to evaluate the intersection control model on: 1) an isolated intersection, and 2) a network of intersections along an arterial. The complete model was then tested and evaluated on the Alton Parkway/I-405 corridor network in Irvine, California. In testing the optimal control model, we simulated a variety of conditions on the freeway and arterial subsystems that cover the range of demand from peak to non-peak, incident to non-incident, conditions. The results of these experiments were evaluated against full-actuated operation and found to offer improved performance.

17. KEY WORDS	18. DISTRIBUTION STATEMENT	
Adaptive Traffic Control, Corridor Management, Mathematical Modeling, Optimal Control	No restrictions. This document is available to the public through the National Technical Information Service, Springfield, VA 22161	
19. SECURITY CLASSIFICATION (of this report)	20. NUMBER OF PAGES	21. PRICE
None	59	N/A

DISCLAIMER STATEMENT

This document is disseminated in the interest of information exchange. The contents of this report reflect the views of the authors who are responsible for the facts and accuracy of the data presented herein. The contents do not necessarily reflect the official views or policies of the State of California or the Federal Highway Administration. This publication does not constitute a standard, specification or regulation. This report does not constitute an endorsement by the Department of any product described herein.

For individuals with sensory disabilities, this document is available in Braille, large print, audiocassette, or compact disk. To obtain a copy of this document in one of these alternate formats, please contact: the Division of Research and Innovation, MS-83, California Department of Transportation, P.O. Box 942873, Sacramento, CA 94273-0001.

Table of Contents

List of Figures

List of Tables

Abstract

This research develops and tests, via microscopic simulation, a real-time adaptive control system for corridor management in the form of three real-time adaptive control strategies: intersection control, ramp control and an integrated control that combines both intersection and ramp control.

The development of these strategies is based on a mathematical representation that describes the behavior of traffic flow in corridor networks and actuated controller operation. Only those parameters commonly found in modern actuated controllers (e.g., Type 170 and 2070 controllers) are considered in the formulation of the optimal control problem. As a result, the proposed strategies easily could be implemented with minimal adaptation of existing field devices and the software that controls their operation.

Microscopic simulation was employed to test and evaluate the performance of the proposed strategies in a calibrated network. Simulation results indicate that the proposed strategies are able to increase overall system performance and also the local performance on ramps and intersections. Prior to testing the complete model, separate tests were conducted to evaluate the intersection control model on: 1) an isolated intersection, and 2) a network of intersections along an arterial. The complete model was then tested and evaluated on the Alton Parkway/I-405 corridor network in Irvine, California.

In testing the optimal control model, we simulated a variety of conditions on the freeway and arterial subsystems that cover the range of demand from peak to non-peak, incident to non-incident, conditions. The results of these experiments were evaluated against full-actuated operation and found to offer improved performance.

Key Words: Adaptive Traffic Control, Corridor Management, Mathematical Modeling, Optimal Control

Executive Summary

This project developed and tested, via microscopic simulation, a real-time adaptive control system for corridor management. Although the focus of the development is on signal controllers designed for operation on arterial street networks, the formulation of the adaptive control strategy explicitly includes interaction with freeway ramp control devices, which are also designed to react adaptively to both the onramp flow, as determined by the operation of adjacent intersection signal controllers, and the traffic state on the mainline freeway. The resulting control strategy is based on a mathematical representation that describes the behavior of real-life processes (traffic flow in corridor networks and actuated controller operation). In formulating the optimal control problem, we have restricted our attention to control of only those parameters commonly found in modern actuated controllers (e.g., Type 170 and 2070 controllers). By doing this, we hope to ensure that the procedures developed herein can be implemented with minimal adaptation of existing field devices and the software that controls their operation.

In the methodological approach taken, we assume that the traffic arrival pattern can be represented as a queue with Poisson arrivals, and from queuing theory we first develop estimates of both the effective green time (equal to actual displayed green interval), and the vehicle arrival flow, departure number and spillovers for the expired signal phase based on the known controller parameter settings. Similarly, we estimate upstream contributions to the target intersections from known parameters at the upstream intersections and readouts from the corresponding signal displays. Dynamic turning fractions at the target intersection, which cannot be known *a priori*, are estimated based on a moving average model.

Maximum green settings provide constraints for the decision of optimal phase splits, which are determined by solving a non-linear optimization problem with the objective to be minimizing total intersection control delay per cycle. The expression used for delay is a generalization of the well-known Webster formulation. These optimized phase splits are used to determine optimal phase minimum green and passage settings.

The outputs of the adaptive control model for intersection signalization are the product of a stochastic optimal control problem that returns dynamic values for the three parameters of actuated controllers—phase minimum green parameter (subject to its absolute minimum based on such other conditions as pedestrian waiting time and start-up lost time), phase passage parameter and phase maximum green parameter—that control its responsiveness to stochastic fluctuations in traffic conditions (other parameters, e.g., yellow interval, clearance interval, phase sequencing, are determined principally in regard to safety and geometric considerations); contrasted to current controller operation, in which these parameters are static/preset, in our formulation they are dynamically set in response to estimates of demand.
Three real-time adaptive control strategies: an intersection control, ramp control and an integrated control that combines both intersection and ramp control are proposed. Microscopic simulation was employed to test and evaluate the performance of the proposed strategies in a calibrated network. Prior to testing the complete model, separate tests were conducted to evaluate the intersection control model on: 1) an isolated intersection, and 2) a network of intersections along an arterial. The complete model was then tested and evaluated on the Alton Parkway/I-405 corridor network in Irvine, California. In testing the optimal control model, we

simulated a variety of conditions on the freeway and arterial subsystems that cover the range of demand from peak to non-peak, incident to non-incident, conditions. The results of these experiments were evaluated against full-actuated operation and found to offer improved performance.

Simulation results indicate that the proposed strategies are able to increase overall system performance and also the local performance on ramps and intersections.

1. Introduction

The objective of this project is to develop and test, via microscopic simulation, a real-time adaptive control system for corridor management. Although the focus of the development is on signal controllers designed for operation on arterial street networks, the formulation of the adaptive control strategy explicitly includes interaction with freeway ramp control devices, which are also designed to react adaptively to both the onramp flow, as determined by the operation of adjacent intersection signal controllers, and the traffic state on the mainline freeway. The proposed control strategy is based on a mathematical representation that describes the behavior of real-life processes (traffic flow in corridor networks and actuated controller operation). In formulating the optimal control problem, we have restricted our attention to control of only those parameters commonly found in modern actuated controllers (e.g., Type 170 and 2070 controllers). By doing this, we hope to ensure that the procedures developed herein can be implemented with minimal adaptation of existing field devices and the software that controls their operation.

A typical advantage of an adaptive signal controller is that, in the case of intersection control, the cycle length, phase splits, and even the phase sequence, may vary from cycle to cycle, in a manner that satisfies the demands of the current traffic pattern. To some extent, actuated controllers are themselves "adaptive" in the sense that they vary these same outcomes, but do so subject to a set of predefined, fixed, parameters that do not "adapt" to current conditions. For the functionality of truly adaptive controllers, a set of on-line optimized phasing and timing parameters are needed.

Existing adaptive controls, such as SCOOT (Robertson and Bretherton, 1991), make incremental adjustments to the current signal plan for the next cycle, in response to the changing traffic demands. In another real-time network control, SCATS (Lowrie, 1992; Sims, 1979), the local-level intersection controller decides its timing parameters on the basis of the degree of saturation, and then incrementally adjusts to varying traffic conditions. The major drawback of these systems is that they are not proactive and therefore, cannot accommodate significant transients effectively. RHODES^{TM}, a real-time traffic-adaptive signal control system developed at the University of Arizona, uses a traffic flow arrivals algorithm – PREDICT (Head, 1995) – to improve effectiveness when calculating online phase timings. In the PREDICT algorithm, detector information on approaches of every upstream intersection, together with the traffic state (arrival and queues), and control plan for the upstream signals are used to predict future traffic volume. It assumes that all surrounding upstream intersections have fixed-time signalized planning, an assumption that is violated in virtually every modern system.

In none of these previous systems do the embedded traffic flow prediction models fully utilize available detector information and control features. Consequently, their applicability is confined only to particular factors, and thus restricted in achieving comprehensively good performance. For any signalized intersection, at least three kinds of information—vehicle actuated detector information, signal timing plan and current signal phase information—can be exploited to infer a relatively rich body of information that can be used in adapting the operation of the signal controller to current, or expected, conditions. Here, we develop a traffic flow prediction model

based on the actuated phase control strategy and other features, such as phase minimum green parameter, phase passage parameter and phase maximum green parameter, together with related detector information gleaned from actuated-signalized upstream intersections to estimate the future arrivals at downstream intersections. To better utilize all available information, our traffic flow prediction model is divided into an approach volume prediction and the corresponding turning proportion estimation. Based on the time of actuation in the upstream detector of neighboring intersections, together with current signal state and control tactics of the neighboring intersections, the arrival pattern of vehicles is predicted. Then by using the exit/entry passage detector cycle/phase counts in the neighboring intersections, the turning percentage for each movement is estimated. As a result, the model can utilize instantaneous information that is currently available but not used, and thus assist fine-tuning intersection performance without any additional hardware investment.

The development and adoption of adaptive control procedures for signalized intersections have been hampered by two fundamental impediments to their successful implementation—those that are theoretically sound invariably have been specified in terms of parameters and control options that simply are not within the lexicon of control devices and typically involve complex mixed-integer-programming formulations that do not lend themselves to real-time solution, and those that do manipulate parameters employed in modern actuated control devices are based on highly simplified approximations and simplifications to both control response and traffic measurement. Consistent modeling of traffic signal operations inevitably includes some sort of conditional piece-wise functions in the mathematical representation. For example, such a representation is the basis of the dispersion-and-store model where the inflow to a link is dispersed and is subsequently stored at its end if the signal at the adjacent intersection is “Red,” or the similar store-and-forward model where the inflow is assumed to travel at a constant travel time, a general relationship of the corresponding outflow discharge would be described by a function that is conditional on the signal indication and the prevailing traffic conditions. Specifically, the outflow is equal to zero if the signal is “Red”, and equal to the minimum of the flow rate of the stored vehicles and the saturation flow rate if “Green”. Within the context of a mathematical programming problem this function is represented by some sort of constraint(s).

Typically, this task has been approached either by considering specific aspects of the process behavior that narrow the applicability of the model and restrict the insight of the findings, or via its questionable manipulation in the solution procedure of the corresponding problem. For example, when designing optimal signal control strategies for surface street networks based on the store-and-forward model, Singh and Tamura (1974), D'Ans and Gazis (1976), and Papageorgiou (1995) assumed that oversaturated conditions prevail. The control variables are the green per cycle ratios given a cycle of fixed duration, so that the outflow discharge is calculated as the product of the saturation flow rate and the green per cycle ratio. In their formulations, traffic signal operation is not explicitly modeled, and the oversaturation assumption restricts the applicability of the control strategy that of a single-ring, 2-phase, fixed cycle controller. As another example, Chang *et al*. (1994) develop signal control strategies for mixed surface street/freeway networks by manipulating the outflow discharge function based on the values of the current state and the previously determined control variable, with the solution algorithm assigning the minimum of the two arguments to the link outflow. In other cases, the conditional

piece-wise function is expressed in the form of minimum or maximum operators; see, e.g., Stephanedes and Chang (1993), and Ziliaskopoulos (2000).

Despite the theoretical consistency of optimal control formulations based on such piece-wise functions, the impracticality of their solution in real-time and their general inconsistency with the operation of existing control devices (e.g., by specifying control transition commands that cannot be understood by existing controller logic) have rendered their practical implementation virtually impossible. In the approach taken herein, we avoid this pitfall by formulating the optimal control problem for a signalized intersection in terms of parameters (phase minimum green parameters, phase passage parameters and phase maximum green parameters) featured in any modern actuated controller, based on a theoretically consistent model of stochastic traffic flow.

2. Methodological Approach

2.1 Intersection control module

In the approach taken here, we assume that the traffic arrival pattern can be represented as a queue with Poisson arrivals, and from queuing theory (e.g., Cox and Smith, 1961) first develop estimates of both the effective green time (equal to actual displayed green interval), and the vehicle arrival flow, departure number and spillovers for the expired signal phase based on the known controller parameter settings. Similarly, we estimate upstream contributions to the target intersections from known parameters at the upstream intersections (a total of four) and readouts from the corresponding signal displays; depending on the expected travel time from the contributing intersection, these values may be drawn from a completed cycle or from an ongoing cycle of operation that commenced just prior to the forecast period for the target intersection. Dynamic turning fractions at the target intersection, which cannot be known *a priori*, are estimated based on a moving average model.

Based on maximum cycle length restrictions, we set phase maximum green parameters based on Webster's functions, accounting for any spillover from previous cycles of operation. These maximum green settings provide constraints for the decision of optimal phase splits, which are determined by solving a non-linear optimization problem with the objective to be minimizing total intersection control delay per cycle. The expression for delay is given by Darroch (1964), which is a generalization of the well-known Webster formulation. These optimized phase splits are used to determine optimal phase minimum green and passage settings. All these timing parameters will be used for the upcoming control cycle as well as provide signal timing data for further optimizations.

As specified, the outputs of the adaptive control model for intersection signalization are the product of a stochastic optimal control problem that returns dynamic values for the three parameters of actuated controllers—phase minimum green parameter (subject to its absolute minimum based on such other conditions as pedestrian waiting time and start-up lost time), phase passage parameter and phase maximum green parameter—that control its responsiveness to stochastic fluctuations in traffic conditions (other parameters, e.g., yellow interval, clearance interval, phase sequencing, are determined principally in regard to safety and geometric

considerations); contrasted to current controller operation, in which these parameters are static/preset, in our formulation they are dynamically set in response to estimates of demand.

2.2 Ramp meter control model

Based on the procedures described in Section 4, below, real-time approach volumes (demand) at the entry ramps downstream of the intersections that feed the ramps are estimated. Owing to the proximity of the intersections to the respective ramp meters, the arrival pattern at the point of metering will be determined using platoon dispersion principles. The departure pattern will be determined as an output of the ramp control model, which will have as its control parameter the instantaneous metering headway, subject to certain installation parameters (e.g., queue override headway, merge queue override headway), and to controller operation protocol.

Caltrans Type 170 metering controllers comprise a number of control elements based on inductive loop detector data inputs. A typical freeway configuration is shown in Figure 1.

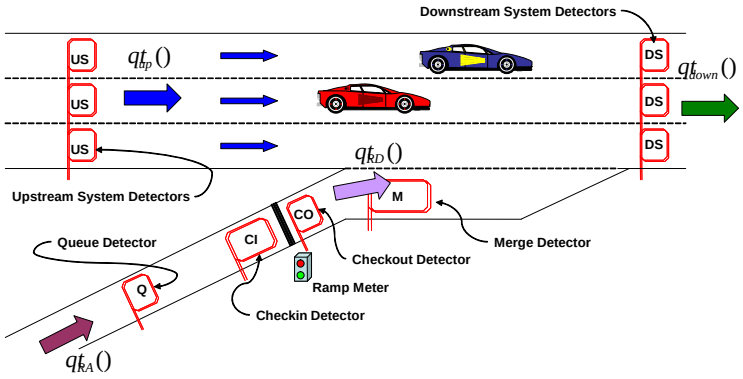

Figure 1. Typical Ramp Metering Configuration

Under current deployment, the headway component of the signal controller uses input from: 1) the upstream detector station, 2) the downstream detector station, 3) the excessive queue detector, and 4) the merge detector station. Basically, the upstream and downstream detectors are used to calculate an appropriate metering headway based on conditions on the mainline freeway, while the queue and merge detectors are used to override the calculated headway based on conditions on the ramp. The actual ramp signal sequencing is determined by input from the demand (Checkin) detector and the passage (Checkout) detector.

A typical open-loop control operation is shown in Figure 2 below, in which the objective of the control is to keep the total demand downstream at a value that does not exceed the capacity downstream:

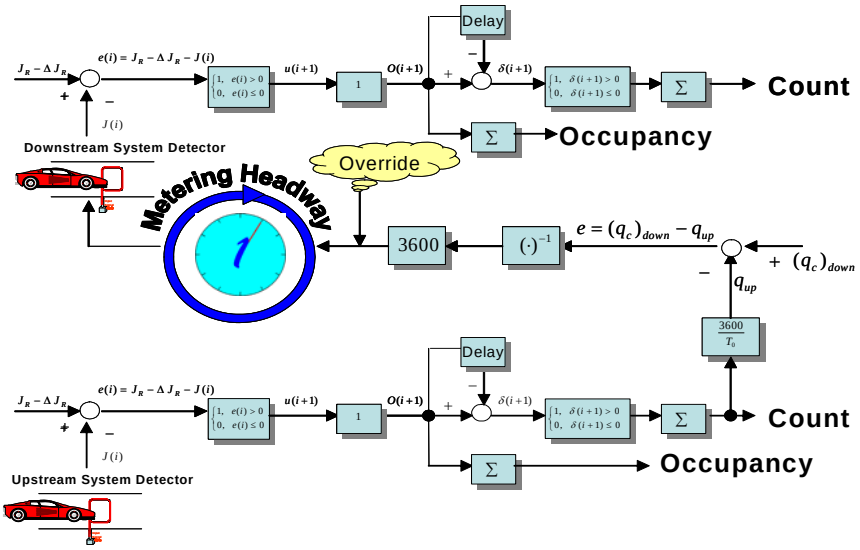

Figure 2. Typical Open-loop Ramp Metering Control

In this controller, the reference input is the downstream capacity, $(q_c)_{down}$, and the metering headway is computed as the headway corresponding to a ramp flow rate that would lead to the total downstream demand being less than or equal to capacity. Note that in this open loop design, the downstream detectors are not used; only the upstream flow rate (which is external to the control system) is utilized.

An example of a simple closed-loop control system is shown in Figure 3 in which the objective is to maintain the downstream speed at a certain prescribed level, $\dot{x}_{REF}$.

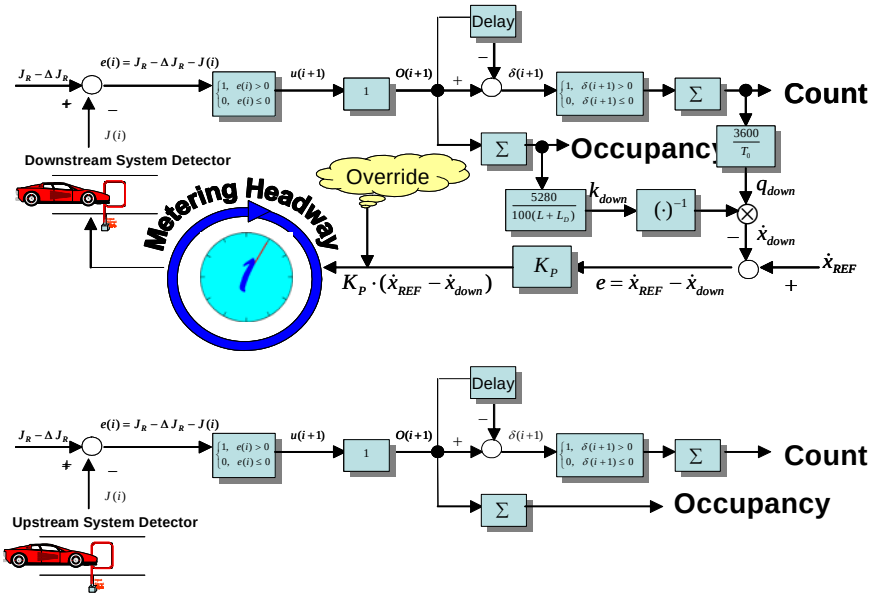

Figure 3. Typical Closed-loop Ramp Metering Control

In this controller, the count and occupancy from the downstream detector stations are used to compute an estimate of the downstream speed, which is then compared to the input reference speed; a proportional control is then used to calculate the ramp metering headway. In this application the upstream system detectors are not used.

In neither of these typical installations is the system-wide performance an explicit consideration in the setting of parameters under which ramp meter controllers operate. In the work presented here, we formulate the ramp control element of our real-time adaptive control corridor model under assumptions of stochastic queuing, with demand input determined from the output of the associated intersection discharge model, and with output determined in accordance with minimizing the delay to the combined corridor system, comprised of: intersection delay, ramp delay, and freeway delay.

2.3 Freeway model

It is well-known that there is an inherent relationship among the speed (and, correspondingly, delay), flow, and density of traffic on a freeway (often referred to as the "fundamental diagram of traffic flow"). Less well-known is the exact form of this relationship. For analytical formulations, such as ours, it is nonetheless necessary to impose a mathematically tractable relationship. Although a number of such relationships have been proposed, based on their mathematical simplicity (see, e.g., Greenshield's linear model), few of these are consistent with observed data; most of these models predict a gradual decrease in speed (linear, in the case of Greenshield's model) as traffic density increases. In fact, our experience suggests that speed remains relatively constant until we reach a point where there are sufficient numbers of vehicles to cause interference in the traffic stream, resulting in the need or desire among drivers to change lanes, accelerate and brake. At this point, we know that things can quickly deteriorate to "stop-and-go" conditions, i.e., congestion, with a precipitous drop in speed. That is, what we expect to see in the way of a relationship between speed and density is something like that shown in Figure 4 below.

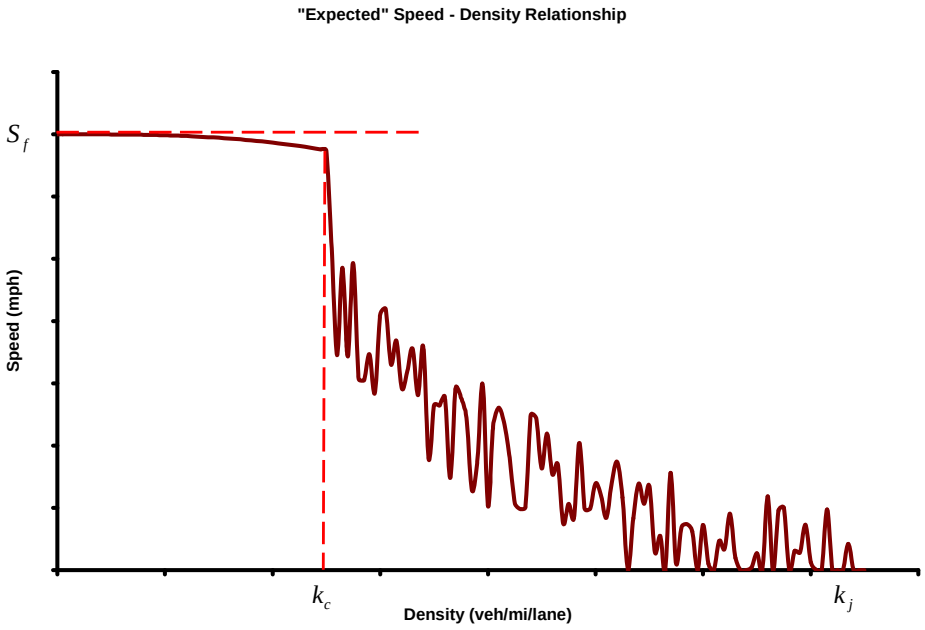

Figure 4. Expected Speed-Density Relationship

This figure depicts a speed–density relationship in which speed remains relatively constant at a value equal to the free-flow speed until we reach capacity, and then speed decreases somewhat unstably from that point to stop-and-go conditions. The corresponding flow–density picture suggests that an underlying theoretical model of the form shown in Figure 5 below (in red) would give results that closely approximate conditions observed in the field. Such a theoretical model would have the attractive feature of being (piecewise) linear (but not smooth, i.e., not having continuous derivatives). Unlike the Greenshield formulation, the linearity here would be in the flow–density relationship, rather than in the speed–density relationship.

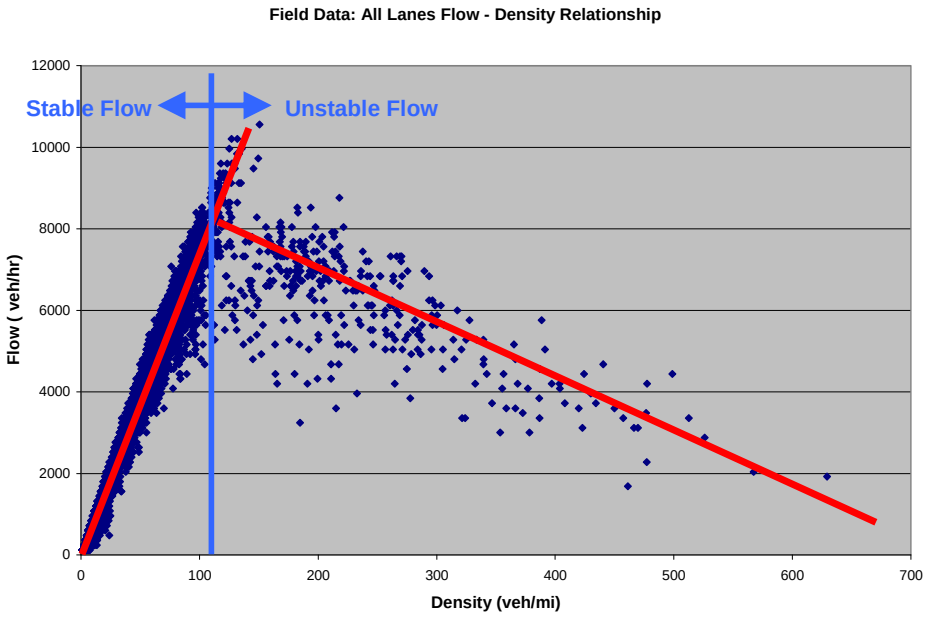

Figure 5. Field Speed-Density Data

Such a model was first proposed by Gordon Newell (of UC Berkeley). Known as the "triangular" flow – density relationship, it has the mathematical form:

$$q = \begin{cases} S_f \cdot k \;\; ; \;\; k \le k_c \\ q_c \cdot \left(1 - \dfrac{k - k_c}{k_j - k_c} \right) \;\; ; \;\; k_j \le k \le k_c \end{cases} \tag{2.1}$$

Since $q = k \cdot \dot{x} \;\; \Rightarrow \;\; \dot{x} = q/k$, the equations above imply the following speed – density relationship for the "triangular" flow – density relationship:

$$\dot{x} = \begin{cases} S_f \;\; ; \;\; k \le k_c \\ \dfrac{S_f}{\dfrac{k_j}{k_c} - 1} \cdot \left(\dfrac{k_j}{k} - 1 \right) \;\; ; \;\; k_j \le k \le k_c \end{cases} \tag{2.2}$$

How closely does the "triangular" flow model replicate field conditions? Below, in Figures 6-11, we superimpose the model results for $S_f = 80$ mph, $q_c = 2{,}300$ veh/hr/lane and $k_j = 211$ veh/mi/lane. (Ordinarily, we would use a formal statistical analysis, such as "least squares regression" to find the best fit, but here we simply pick some values that seem to fit the data.)

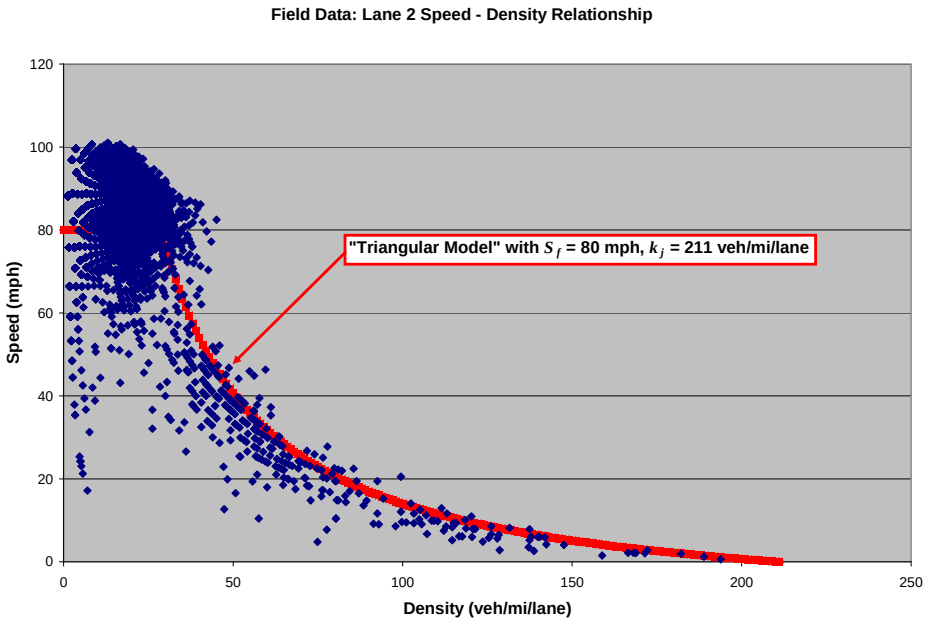

Figure 6. Single Lane Speed-Density Field Data Correspondence with Model

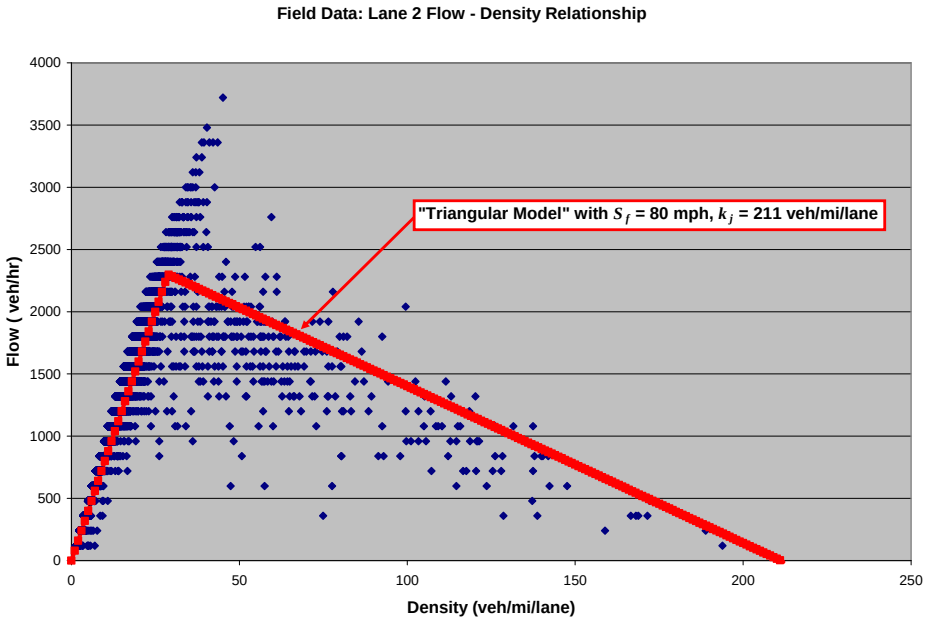

Figure 7. Single Lane Flow-Density Field Data Correspondence with Model

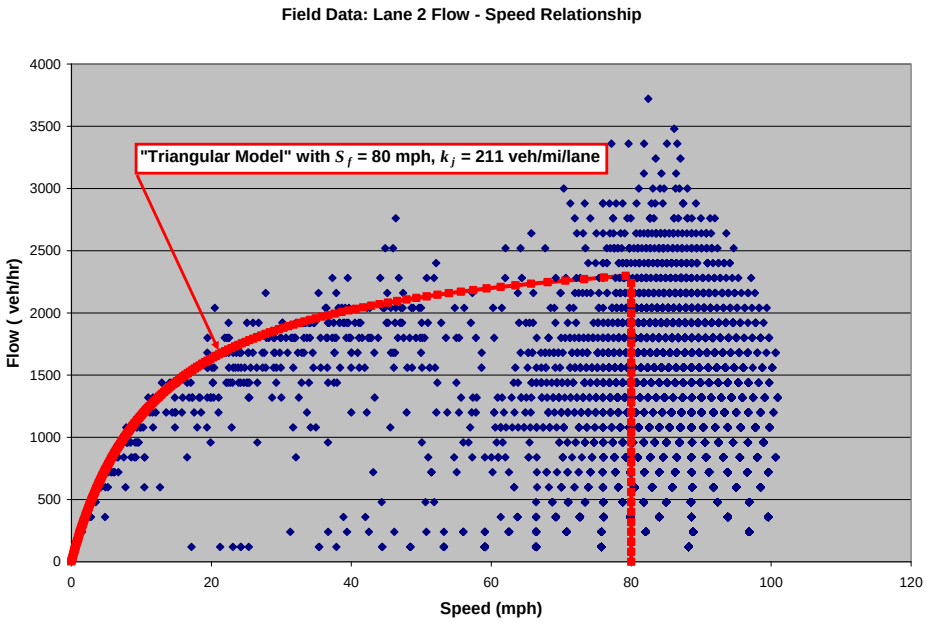

Figure 8. Single Lane Flow-Speed Correspondence with Model

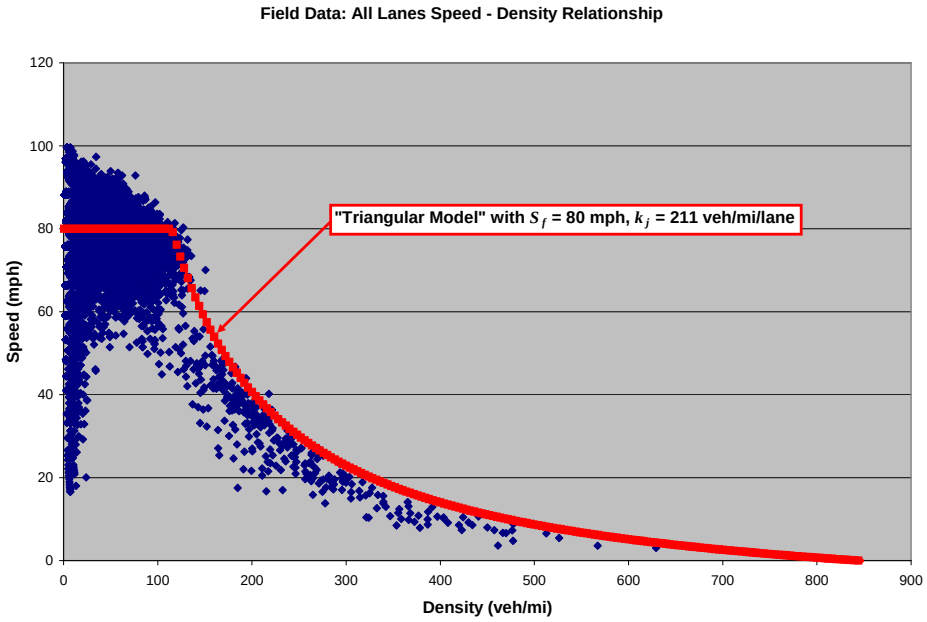

Figure 9. All Lanes Speed-Density Correspondence with Model

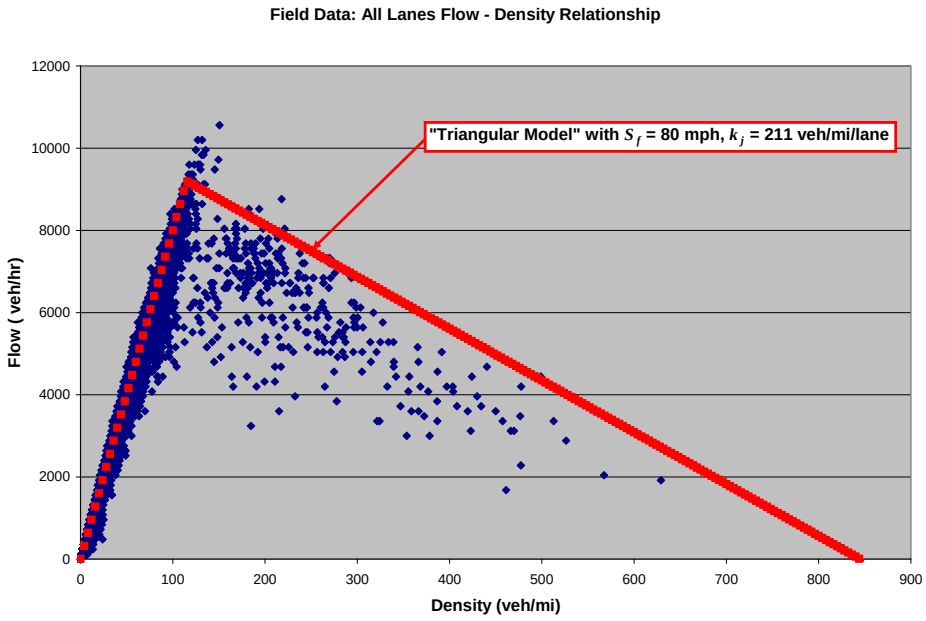

Figure 10. All Lanes Flow-Density Correspondence with Model

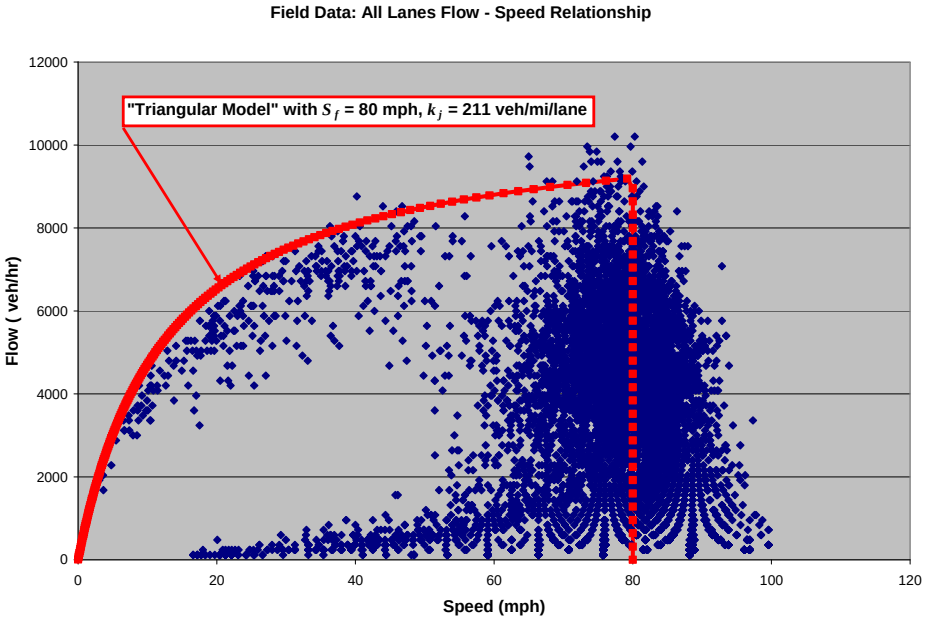

Figure 11. All Lanes Flow-Speed Correspondence with Model

The typical goal for efficient operations is to design a ramp control strategy that processes the maximum number of vehicles, while maintaining uncongested, or "high-speed," conditions. In work conducted herein, we first "fit" the triangular flow model to loop data for each section of the freeway in our corridor. Then, using the calibrated speed-flow-density models, we specify

freeway delay in terms of the mainline volumes (determined from loop stations at the entry boundary to the corridor) and the controlled discharge from the entry ramps within the corridor.

2.4 Optimal corridor control formulation

The procedures outlined in Sections 2.1, 2.2, and 2.3 above specify the total delay components in the corridor network—intersection delay, ramp delay, and freeway delay—in terms of a set of control variables (gap settings, maximum green settings, minimum green settings, and ramp meter headway settings) that can be dynamically adjusted in response to detector inputs and known controller responses. Nominally, these adjustments would be guided by achieving some system optimal condition, e.g., minimization of total system delay, and achieved through solving the accompanying nonlinear optimization problem. For practical application, it is important to recognize that, in most cases, the arterial and freeway/ramp subsystems reside under different jurisdictional control. (For example, in the corridor used as the test network, the arterial/intersection components are under control of the City of Irvine (COI), while the freeway/ramp components are under the control of Caltrans District 12.) We thus specify the system objective as a multi-objective minimization function—minimization of freeway/ramp delay and minimization of arterial signal delay—and develop solutions for optimal control that specify the efficient frontier; i.e., the set of non-dominated control options. In this way, we not only preserve the autonomy of the individual operating agencies, but also are able to present a set of global solutions that translate directly into the recommended set of options for use in CARTESIUS applications.

2.5 Path to deployment

The ultimate goal of this project is to set the stage for deploying a prototype of the optimal corridor control system in a real-world setting for evaluation and testing. It is primarily because of this overriding goal that we have specified the adaptive control procedures solely in terms of those parameters common to existing signal control devices (e.g., Type 170, Type 2070, and NEMA controllers), and utilize only those data provided by inductance loop detectors. As a result, upon successful completion of the adaptive control protocol, its deployment in the field is restricted only by the ability to communicate parameter value updates to the field devices at regular intervals.

To facilitate deployment, our development work is conducted on a corridor network for which we have at least limited authority to conduct tests involving closed-loop control. On the arterial, we have installed a system of Type 2070 controllers at all signalized intersections that operate independently from the local COI system. Work is currently underway to place management of these controllers under CTNet, the latest version of which supports serial and TCP/IP communications; a secondary system based on state-of-the-art Siemens ACTRA Central Traffic Control System with custom-designed Input Acquisition Software is in place as a backup, should the CTNet configuration prove problematic. Software has been developed, and laboratory tested, that permits real-time adaptive control of Caltrans District 12 ramp meters in the study area. We have established real-time communication with these control devices and also receive real-time raw data streams from loop detectors within the study area.

The scope of the current effort includes the development of the corridor adaptive control model and its testing and evaluation in a simulation environment. Prior to testing the complete model, separate tests were conducted to evaluate the intersection control model on: 1) an isolated intersection, and 2) a network of intersections along an arterial. The complete model is then tested and evaluated on the Alton Parkway/I-405 corridor network. Although actual deployment is beyond the scope of the current effort, pending the results of the evaluation of the simulated network, it is envisioned that the adaptive control system can be incorporated as a service within the CARTESIUS deployment under CTNet (in separate, complementary PATH/Caltrans projects).

2.6 Testing and evaluating the proposed control models

In order to test and evaluate the proposed control models, the optimal control formulation has been developed as an API in Paramics. The test network has been drawn for a subsection of the so-called "Irvine Triangle" Paramics network (Figure 12) that has been extensively coded and calibrated as part of the Caltrans ATMS Testbed program.

Figure 12. Irvine Triangle Network

In testing the optimal control model, we simulate a variety of conditions on the freeway and arterial subsystems that cover the range of demand from peak to non-peak, incident to non-incident, conditions. The results of these experiments are evaluated against full-actuated operation (these models have already been coded as API functions within Paramics). In the first phase of the evaluation, we are interested only in the performance of the arterial subsystem, rather than in the combined performance of the freeway-arterial system—this latter aspect of the study is addressed in subsequent testing.

3. Theoretical Development of the Intersection Control Model

3.1 Conceptualization

Consider the dual-ring actuated controller shown in Figure13 below:

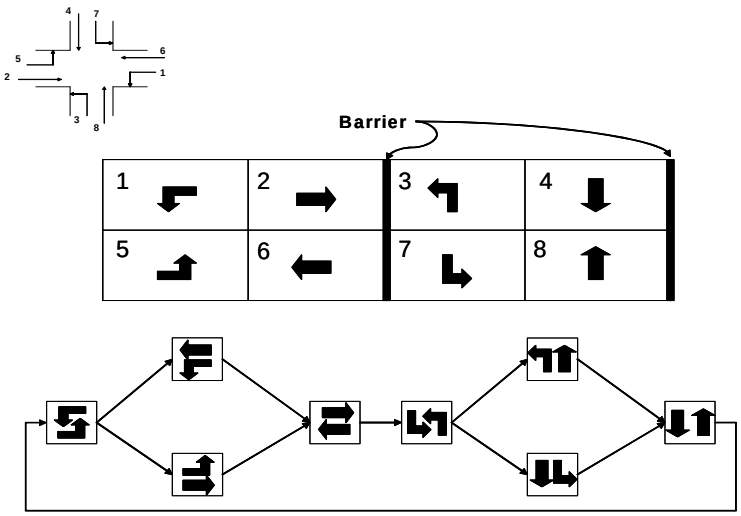

Figure 13. Dual-ring Controller Phasing Diagram

Depending on the values of controller parameters and the traffic arrival pattern, at most six distinct "stages" will be realized; e.g.,

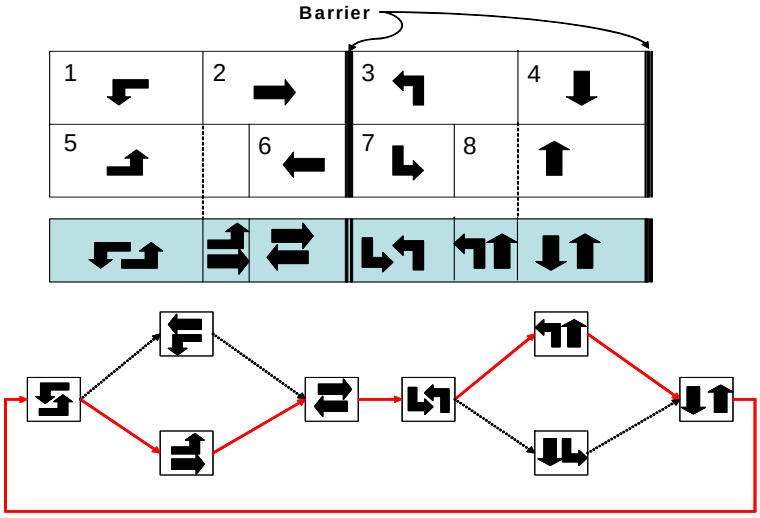

Figure 14. Dual-ring Controller Stages

For the *i* th phase, designate the phase split for the *j* th cycle by G_i^j, and duration of red phase by R_i^j. Then, the complete breakdown of any particular cycle *j* for phase *i* can be represented as follows:

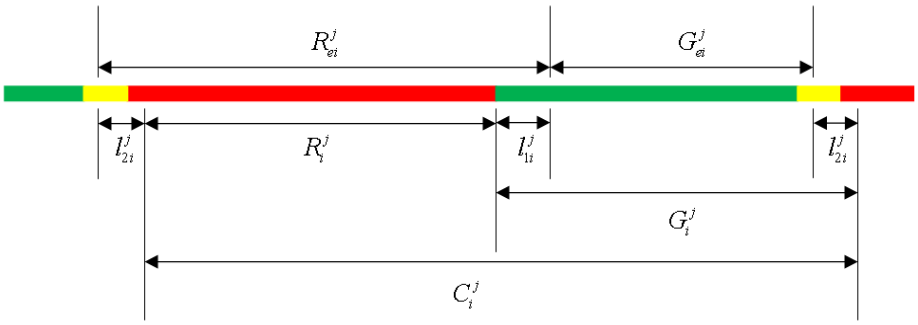

Figure 15. Phase State

In Figure 15:

C_i^j = Cycle length of cycle *j*

l_{1i}^j = Start-up lost time associated with phase *i* during cycle *j*

l_{2i}^j = Clearance lost time associated with phase *i* during cycle *j*

R_{ei}^j = Effective red time associated with phase *i* during cycle *j*

G_{ei}^j = Effective green time associated with phase *i* during cycle *j*

Here we assume that the lost times l_{1i} and l_{2i}, and thus the total lost time L_i, for phase *i* are constant through all cycles, and the effective green, G_{ei}^j, is equal to the actual displayed green. Designating the mean arrival flow rate for phase *i* during cycle *j* by λ_i^j and the constant mean saturation flow rate for phase *i* through all cycles by S_i, the pattern of arrivals/departures for any particular phase *i* is as shown below:

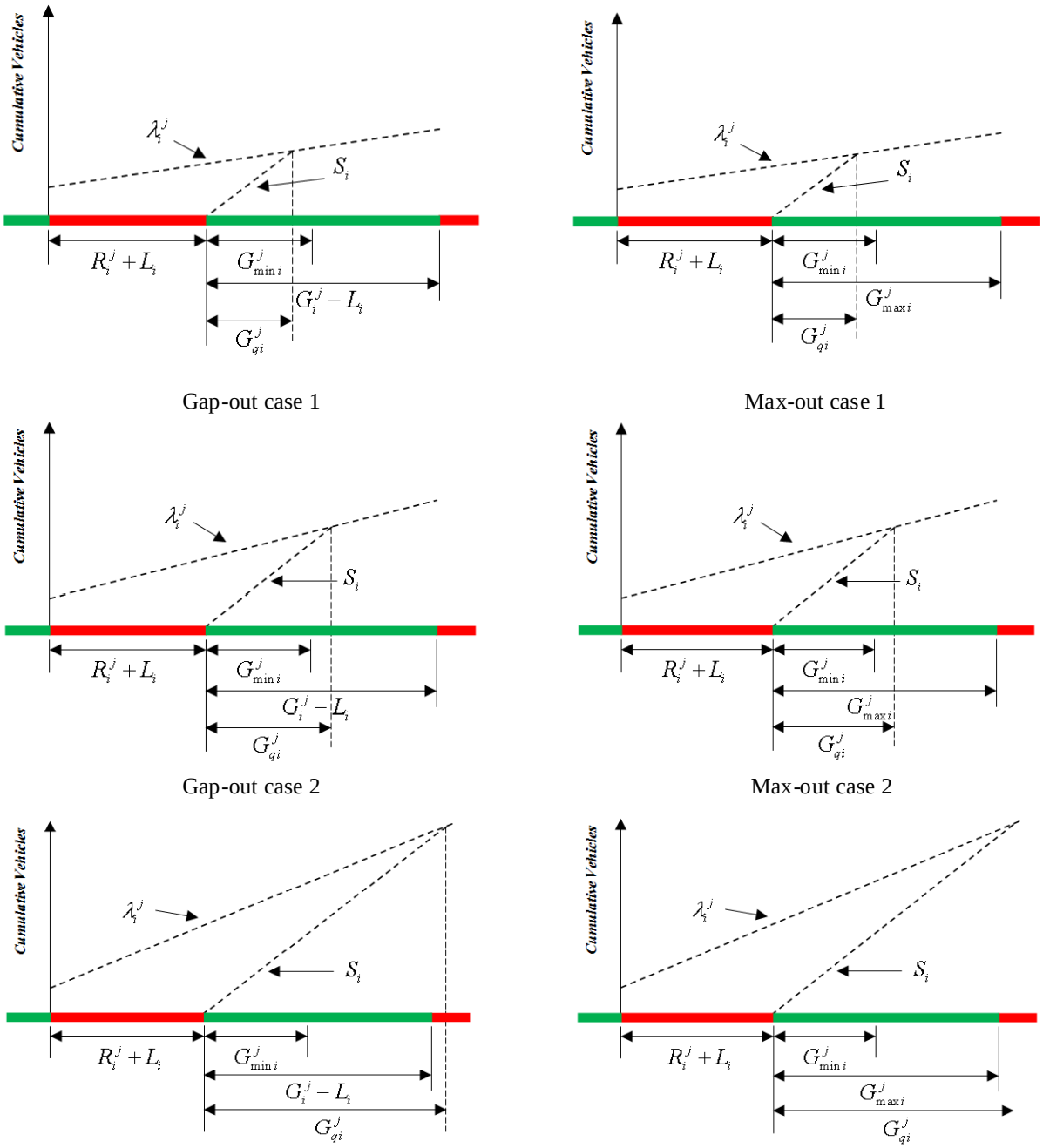

Figure 16. Pattern of Arrivals/Departures

In Figure 16:

$G_{\min i}^j$ = Minimum green time associated with phase *i* during cycle *j*

$G_{\max i}^j$ = Maximum green time associated with phase *i* during cycle *j*

G_{qi}^j = Queue service time associated with phase *i* during cycle *j*

As can be seen, depending on the phase termination mode (either gap-out or max-out) and the values of queue service time, there are six cases that describe distinct arrival/departure patterns.

3.2 Determining vehicle arrival flow rate λ_i^j

The gap-out and max-out situations are considered separately to determine λ_i^j. In gap-out control, the green phase terminates when the vehicle gap (headway) larger than the unit extension (gap setting) occurs. Let β_i^j denote the gap setting for phase *i* during cycle *j*, and Z_i^j the waiting time for the occurrence of the first vehicle gap of at least β_i^j. Based on Poisson arrival process, the associated headway distribution is given by $\phi(t) = \lambda_i^j \exp(-\lambda_i^j t)$. Denote by $\Omega(t)$ the probability density of the delay in waiting for a gap of at least β_i^j. The probability that the first gap is $\geq \beta_i^j$ is then

$$\bar{\alpha}_0 = \int_0^\infty H\left(t - \beta_i^j\right)\phi_0(t)dt \tag{3.1}$$

where $H(\cdot)$ is the Heaviside function.

Then, $\Omega(t)$ is given by

$$\Omega(t) = \bar{\alpha}_0\delta(t) + \Omega_1(t) \tag{3.2}$$

where $\delta(t)$ is the Dirac delta function, and $\Omega_1(t)$ is the contribution due to having to wait for at least one vehicle to pass before a gap of at least β_i^j materializes. The probability that an arbitrary gap is at least β_i^j is given by

$$\bar{\alpha} = \int_0^\infty H\left(t - \beta_i^j\right)\phi(t)dt \tag{3.3}$$

Then

$$\Omega_1(t) = \bar{\alpha} Z_i^j(t) \tag{3.4}$$

where $Z_i^j(t)dt$ is the probability that a vehicle arrives during the time interval $(t, t+dt)$ and no gap of at least β_i^j has been detected up to that point.

Then

$$\Omega(t) = \bar{\alpha}_0 \delta(t) + \bar{\alpha} Z_i^j(t) \tag{3.5}$$

Let

$$\begin{aligned} \Psi_0(t) &= \phi_0(t)\left[1 - H\left(t - \beta_i^j\right)\right] \\ \Psi(t) &= \phi(t)\left[1 - H\left(t - \beta_i^j\right)\right] \end{aligned} \tag{3.6}$$

Then, $\Psi_0(t)dt$ is the probability that the first gap is in the time interval $(t, t+dt)$ and it is not a gap of at least β_i^j, and $\Psi(t)dt$ is the probability that a succeeding gap is in the time interval $(t, t+dt)$ and is not a gap of at least β_i^j. If a vehicle passes at time *t* and no gap of at least β_i^j has materialized, it is either the first vehicle to do so, or the last such event occurred at some time $\tau < t$ and the succeeding gap was not a gap of at least β_i^j. These two possibilities are captured by

$$Z_i^j(t) = \Psi_0(t) + \int_0^t Z_i^j(\tau)\Psi(t-\tau)d\tau \tag{3.7}$$

Denote by

$$f^*(s) = \int_0^\infty e^{-st} f(t)dt \tag{3.8}$$

the Laplace transform of $f(t)$. Then, the transformation of the convolution integral above is

$$Z_i^{j*}(s) = \frac{\Psi_0^*(s)}{1 - \Psi^*(s)} \tag{3.9}$$

But,

$$\Omega^*(s) = \bar{\alpha}_0 + \bar{\alpha} Z_i^{j*}(s) = \bar{\alpha}_0 + \bar{\alpha}\frac{\Psi_0^*(s)}{1 - \Psi^*(s)} \tag{3.10}$$

or,

$$\Omega^*(s) = e^{-\lambda_i^j \beta_i^j} \frac{s + \lambda_i^j}{s + \lambda_i^j e^{-(s+\lambda_i^j)\beta_i^j}} \tag{3.11}$$

Let $\left(\bar{Z}_i^j\right)^n$ denote the *n* th moment of Z_i^j. Then

$$\left(\bar{Z}_i^j\right)^n = \int_0^\infty t^n \Omega(t) dt = (-1)^n \frac{d^n}{ds^n} \Omega^*(s)\Big|_{s=0} \tag{3.12}$$

Then, the expected wait time $E\left(Z_i^j\right)$ for the first gap of at least β_i^j duration is given by

$$E\left(Z_i^j\right) = \frac{\exp\left(\lambda_i^j \beta_i^j\right) - 1}{\lambda_i^j} - \beta_i^j \tag{3.13}$$

Therefore, the phase split can be expressed by

$$G_i^j = L_i + G_{\min i}^j + \frac{\exp\left(\lambda_i^j \beta_i^j\right) - 1}{\lambda_i^j} - \beta_i^j + \beta_i^j = L_i + G_{\min i}^j + \frac{\exp\left(\lambda_i^j \beta_i^j\right) - 1}{\lambda_i^j} \tag{3.14}$$

In Eq. (3.14), all variables except λ_i^j are known signal timing parameters obtained from the expired phase, and thus the vehicle arrival flow rate λ_i^j can be determined by solving the nonlinear inverse function $F^{-1}(\lambda_i^j)$, i.e.,

$$\lambda_i^j = F^{-1}(\lambda_i^j) \tag{3.15}$$

where $F\left(\lambda_i^j\right) = G_i^j - L_i - G_{\min i}^j - \frac{\exp\left(\lambda_i^j \beta_i^j\right) - 1}{\lambda_i^j} = 0$

In max-out-controlled termination of green, arriving vehicles keep actuating the extension detector until maximum green limit is reached. Therefore, it is safe to presume that the number of vehicles arriving from the end of minimum green to the end of phase green is greater than the minimum vehicle arrivals sufficient to invoke max-out conditions, i.e.,

$$\lambda_i^j (G_i^j - L_i - G_{\min i}^j) \geq \frac{G_i^j - L_i - G_{\min i}^j}{\beta_i^j}$$

or,

$$\lambda_i^j \geq \frac{1}{\beta_i^j} \tag{3.16}$$

Specifically, we assume here that λ_i^j is approximately equal to the mean of $1/\beta_i^j$ and S_i, i.e.,

$$\lambda_i^j = \left(\frac{1}{\beta_i^j} + S_i\right) / 2 \tag{3.17}$$

Also, λ_i^j can be determined with the known parameters β_i^j and S_i.

3.3 Determining vehicle departure number $N(G_i^j)$ and spillover ${}^{spill}Q_i^j$

The number of vehicle departures and any spillover depend on the value of queue service time, $\boldsymbol{G_{qi}^j}$. Let $\boldsymbol{Q_i^j}(0)$ denote the queue remaining at the end of the prior green phase and $\boldsymbol{Q_i^j}$ denote the number of arrivals associated with phase *i* during the effective red $\boldsymbol{R_i^j + L_i^j}$. Then $\boldsymbol{G_{qi}^j}$ is the convolution of $\boldsymbol{Q_i^j}(0) + \boldsymbol{Q_i^j}$ busy periods in a queue with Poisson arrivals with rate λ_i^j and constant service time $s_i \left(= 1/S_i\right)$. Then, from queuing theory (e.g., Cox and Smith, 1961, p 55),

$$\boldsymbol{E}\left[\boldsymbol{G_{qi}^j} \mid \left(\boldsymbol{Q_i^j}(0) + \boldsymbol{Q_i^j}\right)\right] = \frac{\left[\boldsymbol{Q_i^j}(0) + \boldsymbol{Q_i^j}\right]\boldsymbol{s_i}}{1 - \boldsymbol{\lambda_i^j s_i}} \tag{3.18}$$

Under the assumption of Poisson arrivals, $\boldsymbol{Q_i^j}$ is Poisson distributed with mean $\lambda_i^j \left(R_i^j + L_i\right)$,

$$\boldsymbol{E}\left(\boldsymbol{G_{qi}^j}\right) = \frac{\left[\boldsymbol{Q_i^j}(0) + \boldsymbol{\lambda_i^j}\left(\boldsymbol{R_i^j} + \boldsymbol{L_i^j}\right)\right]\boldsymbol{s_i}}{1 - \boldsymbol{\lambda_i^j s_i}}$$

or,

$$\boldsymbol{E}\left(\boldsymbol{G_{qi}^j}\right) = \frac{\boldsymbol{Q_i^j}(0) + \boldsymbol{\lambda_i^j}\left(\boldsymbol{R_i^j} + \boldsymbol{L_i^j}\right)}{\boldsymbol{S_i} - \boldsymbol{\lambda_i^j}} \tag{3.19}$$

Referring to the arrival/departure pattern as shown in Figure 16 above, the value of $\boldsymbol{G_{qi}^j}$ may lie in one of three different ranges:

Case 1:

$$\boldsymbol{G_{qi}^j} \le \boldsymbol{G_{\min i}^j}$$

or,

$$\frac{\boldsymbol{Q_i^j}(0) + \boldsymbol{\lambda_i^j}\left(\boldsymbol{R_i^j} + \boldsymbol{L_i^j}\right)}{\boldsymbol{S_i} - \boldsymbol{\lambda_i^j}} \le \boldsymbol{G_{\min i}^j}$$

or,

$$\frac{S_i G^j_{\min i} - Q^j_i(0)}{R^j_i + L_i + G^j_{\min i}} \le \lambda^j_i \tag{3.20}$$

Case 2:

$$G^j_{\min i} < G^j_{qi} \le \left(G^j_i - L_i\right)$$

or,

$$G^j_{\min i} < \frac{Q^j_i(0) + \lambda^j_i\left(R^j_i + L^j_i\right)}{S_i - \lambda^j_i} \le \left(G^j_i - L_i\right)$$

or,

$$\frac{S_i G^j_{\min i} - Q^j_i(0)}{R^j_i + L_i + G^j_{\min i}} < \lambda^j_i \le \frac{S_i(G^j_i - L_i) - Q^j_i(0)}{R^j_i + G^j_i} \tag{3.21}$$

Case 3:

$$G^j_{qi} > \left(G^j_i - L_i\right)$$

or,

$$\frac{Q^j_i(0) + \lambda^j_i\left(R^j_i + L^j_i\right)}{S_i - \lambda^j_i} > \left(G^j_i - L_i\right)$$

or,

$$\lambda^j_i > \frac{S_i(G^j_i - L_i) - Q^j_i(0)}{R^j_i + G^j_i} \tag{3.22}$$

Note that in max-out-controlled termination, $G^j_i - L_i = G^j_{\max i}$.

As can be seen, three consecutive, non-overlapped numerical intervals regarding to the value of λ^j_i are illustrated by inequalities (3.20), (3.21) and (3.22), which are also expressed in terms of known timing parameters. Based on the λ^j_i determined by Eq. (3.15) or Eq. (3.17), only one inequality (i.e., only one case) is "true" for the gap-out or max-out situation. Hence, the vehicle departure number during the phase split, $N(G^j_i)$, and spillover ${}^{spill}Q^j_i$ can be determined by the following equations that correspond to the true case.

Case 1 or 2:

$$N(G_i^j) = S_i G_{qi}^j + \lambda_i^j \left(G_i^j - L_i - G_{qi}^j \right)$$

or,

$$N(G_i^j) = \left(S_i - \lambda_i^j \right) G_{qi}^j + \lambda_i^j \left(G_i^j - L_i \right)$$

or,

$$N(G_i^j) = \left(S_i - \lambda_i^j \right) \frac{\left[Q_i^j(0) + \lambda_i^j \left(R_i^j + L_i \right) \right]}{S_i - \lambda_i^j} + \lambda_i^j \left(G_i^j - L_i \right)$$

or,

$$N(G_i^j) = Q_i^j(0) + \lambda_i^j \left(G_i^j + R_i^j \right) \tag{3.23}$$

And,

$${}^{spill}Q_i^j = Q_i^j(0) + \lambda_i^j \left(G_i^j + R_i^j \right) - N(G_i^j)$$

or,

$${}^{spill}Q_i^j = 0 \tag{3.24}$$

Case 3:

$$N(G_i^j) = S_i \left(G_i^j - L_i \right) \tag{3.25}$$

And,

$${}^{spill}Q_i^j = Q_i^j(0) + \lambda_i^j \left(G_i^j + R_i^j \right) - N(G_i^j)$$

Or,

$${}^{spill}Q_i^j = Q_i^j(0) + \lambda_i^j \left(G_i^j + R_i^j \right) - S_i \left(G_i^j - L_i \right) \tag{3.26}$$

For Eq. (3.23) to Eq. (3.26), $N(G_i^j)$ and ${}^{spill}Q_i^j$ can be determined with such known parameters obtained from the expired phase as $\boldsymbol{Q_i^j}(0)$, G_i^j, R_i^j and λ_i^j.

3.4 Determining future vehicle arrival flow rate λ_i^{j+1}

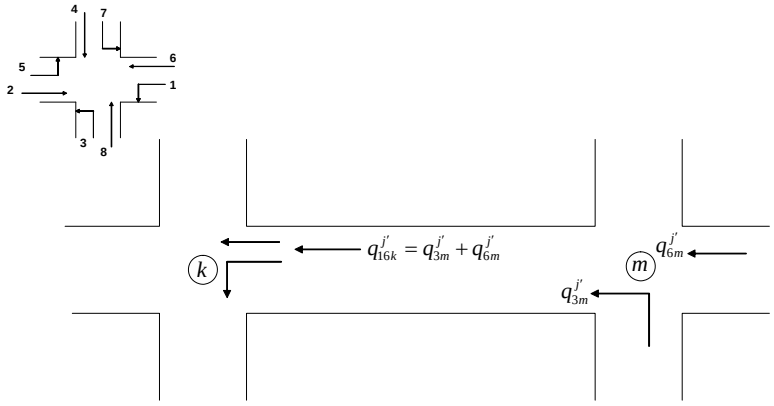

Figure 17. Approach Volumes

at intersection *m* during cycle j'.

$$E(q_{im}^{j'}) = N(G_{im}^{j'}) / C_m^{j'} \tag{3.27}$$

where

$$C^{j'} = G_1^{j'} + G_2^{j'} + G_3^{j'} + G_4^{j'} \quad \text{or} \quad C^{j'} = G_5^{j'} + G_6^{j'} + G_7^{j'} + G_8^{j'}$$

Therefore,

$$E(q_{rsk}^{j'}) = E(q_{tm}^{j'}) + E(q_{um}^{j'}) \;;\; rstu = 1636, 2527, 3858, 4714 \tag{3.28}$$

where intersection *m* is on the respective upstream approach to the phase [1,6], [2,5], [3,8],and [4,7] movements at intersection *k*.

And, the turning fractions for cycle *j* can be expressed as

$$TF_{ik}^{j} = \frac{\lambda_{ik}^{j}}{\lambda_{ik}^{j} + \lambda_{rk}^{j}} \;;\; ir = 16, 25, 38, 47, 61, 52, 83, 74 \tag{3.29}$$

where TF_{ik}^{j} denotes the percent of traffic on the approach contributing to phase *i* that is assigned to phase *i* during cycle *j*.

Next, forecast TF_{ik}^{j+1} by some form of "moving average" model; e.g.,

$$TF_{ik}^{j+1} = \sum_{n=j-j_o}^{j} \alpha_n \cdot TF_{ik}^{n} \;;\; \alpha_j \geq \alpha_{j-1} \geq \ldots \geq \alpha_{j-j_o} \;\; ; \;\; \sum_{n=j-j_o}^{j} \alpha_n = 1 \tag{3.30}$$

Then, compute λ_{ik}^{j+1} , $i = 1,\ldots,8$ as

$$\lambda_{ik}^{j+1} = TF_{ik}^{j+1} \cdot q_{irk}^{j'} \ , \ ir = 16, 25, 38, 47$$
$$\lambda_{rk}^{j+1} = TF_{rk}^{j+1} \cdot q_{irk}^{j'} \ , \ ir = 16, 25, 38, 47$$

3.5 Determining optimal maximum green $G_{\max i}^{j+1}$

Here, we determine maximum green using Webster's formulas, i.e.,

$$D_i^{j+1} = \left[\lambda_i^{j+1} + \left(3600 / C_{\max}\right) Q_i^{j+1}(0) \right] \Big/ S_i \tag{3.31}$$

where

$C_{\max} =$ Maximum allowable cycle length , say 120 seconds

$$Q_i^{j+1}(0) = {}^{spill}Q_i^j \tag{3.32}$$

The term $\left(3600 / C_{\max}\right) Q_i^{j+1}(0)$ represents an approximation of the equivalent apparent arrival rate (per hour) due to incorporating the leftover queue from the previous cycle (i.e., ${}^{spill}Q_i^j$) present at onset of green. And, the critical path through each ring is determined by

Left Side Conditions: Critical Path = $i^* m^* \ni D_{i^*}^{j+1} + D_{m^*}^{j+1} = \underset{i\,m=12,56}{Max} \left(D_i^{j+1} + D_m^{j+1} \right)$

Right Side Conditions: Critical Path = $r^* n^* \ni D_{r^*}^{j+1} + D_{n^*}^{j+1} = \underset{r\,n=34,78}{Max} \left(D_r^{j+1} + D_n^{j+1} \right)$ (3.33)

Employing Webster's optimal distribution of green, we obtain for the left and right portions of the ring, ${}^{Web}G_{left}^{j+1}$ and ${}^{Web}G_{right}^{j+1}$, respectively,

$$\begin{aligned} {}^{Web}G_{left}^{j+1} &= \frac{D_{i^*}^{j+1} + D_{m^*}^{j+1}}{\left(D_{i^*}^{j+1} + D_{m^*}^{j+1}\right) + \left(D_{r^*}^{j+1} + D_{n^*}^{j+1}\right)} \cdot \left[C_{\max} - \left(L_{i^*} + L_{m^*} + L_{r^*} + L_{n^*} \right) \right] \\ {}^{Web}G_{right}^{j+1} &= \frac{D_{r^*}^{j+1} + D_{n^*}^{j+1}}{\left(D_{i^*}^{j+1} + D_{m^*}^{j+1}\right) + \left(D_{r^*}^{j+1} + D_{n^*}^{j+1}\right)} \cdot \left[C_{\max} - \left(L_{i^*} + L_{m^*} + L_{r^*} + L_{n^*} \right) \right] \end{aligned} \tag{3.34}$$

Using the same philosophy, we calculate for the critical movements:

$$
\begin{aligned}
{}^{Web}G_i^{j+1} &= \frac{D_{i^*}^{j+1}}{\left(D_{i^*}^{j+1} + D_{m^*}^{j+1}\right)} \cdot {}^{Web}G_{left}^{j+1} \\
{}^{Web}G_m^{j+1} &= \frac{D_{m^*}^{j+1}}{\left(D_{i^*}^{j+1} + D_{m^*}^{j+1}\right)} \cdot {}^{Web}G_{left}^{j+1} \\
{}^{Web}G_r^{j+1} &= \frac{D_{r^*}^{j+1}}{\left(D_{r^*}^{j+1} + D_{n^*}^{j+1}\right)} \cdot {}^{Web}G_{right}^{j+1} \\
{}^{Web}G_n^{j+1} &= \frac{D_{n^*}^{j+1}}{\left(D_{r^*}^{j+1} + D_{n^*}^{j+1}\right)} \cdot {}^{Web}G_{right}^{j+1}
\end{aligned}
\qquad (3.35)
$$

And, for the non-critical movements:

$$
\begin{aligned}
{}^{Web}G_i^{j+1} &= \frac{D_i^{j+1}}{\left(D_i^{j+1} + D_m^{j+1}\right)} \cdot {}^{Web}G_{left}^{j+1} \; ; im = 12,56 \; ; im \neq i^* m^* \\
{}^{Web}G_m^{j+1} &= \frac{D_m^{j+1}}{\left(D_i^{j+1} + D_m^{j+1}\right)} \cdot {}^{Web}G_{left}^{j+1} \; ; \; im = 12,56 \; ; im \neq i^* m^* \\
{}^{Web}G_r^{j+1} &= \frac{D_r^{j+1}}{\left(D_r^{j+1} + D_n^{j+1}\right)} \cdot {}^{Web}G_{right}^{j+1} \; ; r\,n = 34,78 \; ; r\,n \neq r^* n^* \\
{}^{Web}G_n^{j+1} &= \frac{D_n^{j+1}}{\left(D_r^{j+1} + D_n^{j+1}\right)} \cdot {}^{Web}G_{right}^{j+1} \; ; r\,n = 34,78 \; ; r\,n \neq r^* n^*
\end{aligned}
\qquad (3.36)
$$

Then, set maximum greens according to Webster's optimal phase splits

$$G_{\max i}^{j+1} = {}^{Web}G_i^{j+1} \; ; \; i = 1,\ldots,8$$

3.6 Determining optimal phase split G_i^{j+1}

A nonlinear optimization problem is formulated to determine optimal phase splits, with the objective to be minimizing total intersection control delay during the upcoming cycle. The optimization of phase splits is also called "Critical Intersection Control (CIC)" and it is considered a first generation UTCS control strategy; our formulation of this strategy explicitly incorporates stochastic factors incorporated with optimal control. The delay expression is given by Darroch (1964), which is a generalization of the well-known Webster formulation,

$$E\left(W_i^{j+1}\right) = \frac{\lambda_i^{j+1}}{2(1-\lambda_i^{j+1}s_i)}\left\{(R_i^{j+1})^2 + R_i^{j+1}\left(\frac{2}{\lambda_i^{j+1}}Q_i^{j+1}(0) + s_i\left[1+\frac{1}{1-\lambda_i^{j+1}s_i}\right]\right)\right\} \; ; \; i = 1,2,\ldots,8$$

or,

$$E\left(W_i^{j+1}\right)=\frac{S_i\lambda_i^{j+1}}{2(S_i-\lambda_i^{j+1})}\left\{(R_i^{j+1})^2+R_i^{j+1}\left(\frac{2}{\lambda_i^{j+1}}Q_i^{j+1}(0)+\frac{1}{S_i}+\frac{1}{S_i-\lambda_i^{j+1}}\right)\right\};\ i=1,2,\ldots,8 \tag{3.37}$$

where W_i^{j+1} is the waiting time per cycle. The optimization problems can be expressed by

$$Min\sum_{i=1}^{8}E\left(W_i^{j+1}\right) \tag{3.38}$$

Based on the circular dependency relationship in dual-ring structure as shown in Figure 18, the term R_i^{j+1} can be expressed as

$$\begin{aligned}
R_1^{j+1}&=G_2^j+G_3^j+G_4^j\\
R_2^{j+1}&=G_3^j+G_4^j+G_1^{j+1}\\
R_3^{j+1}&=G_4^j+G_1^{j+1}+G_2^j\\
R_4^{j+1}&=G_1^{j+1}+G_2^{j+1}+G_3^{j+1}\\
R_5^{j+1}&=G_6^j+G_7^j+G_8^j\\
R_6^{j+1}&=G_7^j+G_8^j+G_5^{j+1}\\
R_7^{j+1}&=G_8^j+G_5^{j+1}+G_6^{j+1}\\
R_8^{j+1}&=G_5^{j+1}+G_6^{j+1}+G_7^{j+1}
\end{aligned} \tag{3.39}$$

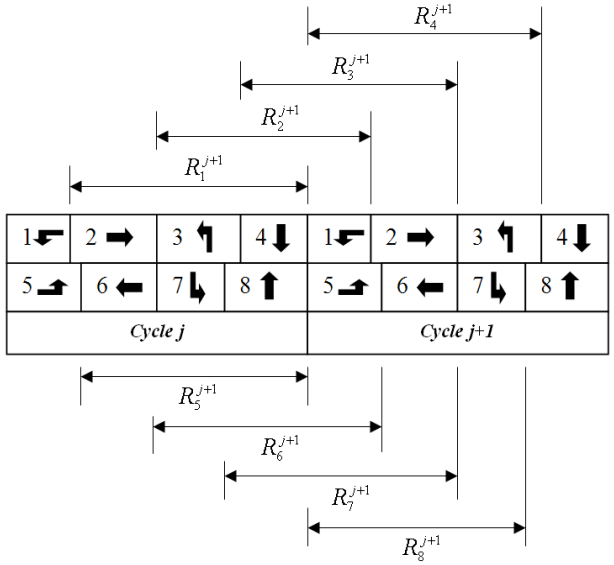

Figure 18. Circular Dependency

We note that Eq. (3.39) does not contain terms G_4^{j+1} and G_8^{j+1}, and thus these two variables cannot be expressed in the optimization problem. Here, a rolling horizon scheme is applied by substituting R_1^{j+1} with R_1^{j+2} , and R_5^{j+1} with R_5^{j+2}, then we have

$$\begin{aligned}
R_1^{j+2} &= G_2^{j+1} + G_3^{j+1} + G_4^{j+1} \\
R_2^{j+1} &= G_3^{j} + G_4^{j} + G_1^{j+1} \\
R_3^{j+1} &= G_4^{j} + G_1^{j+1} + G_2^{j} \\
R_4^{j+1} &= G_1^{j+1} + G_2^{j+1} + G_3^{j+1} \\
R_5^{j+2} &= G_6^{j+1} + G_7^{j+1} + G_8^{j+1} \\
R_6^{j+1} &= G_7^{j} + G_8^{j} + G_5^{j+1} \\
R_7^{j+1} &= G_8^{j} + G_5^{j+1} + G_6^{j+1} \\
R_8^{j+1} &= G_5^{j+1} + G_6^{j+1} + G_7^{j+1}
\end{aligned} \tag{3.40}$$

Then, the optimization problem becomes

$$Min\left[\sum_{i=2,3,4,6,7,8} E\left(W_i^{j+1}\right) + \sum_{r=1,5} E\left(W_r^{j+2}\right)\right] \tag{3.41}$$

In the expression for $E\left(W_r^{j+2}\right)$, i.e.,

$$E\left(W_r^{j+2}\right) = \frac{S_r \lambda_r^{j+2}}{2(S_r - \lambda_r^{j+2})}\left\{(R_r^{j+2})^2 + R_r^{j+2}\left(\frac{2}{\lambda_r^{j+2}} Q_r^{j+2}(0) + \frac{1}{S_r} + \frac{1}{S_r - \lambda_r^{j+2}}\right)\right\};\ r = 1,5$$

we assume $Q_r^{j+2}(0) = 0$, and λ_r^{j+2} can be estimated by some form of "moving average" model, e.g.,

$$\lambda_r^{j+2} = \sum_{n=j+1-j_o}^{j+1} \alpha_n \cdot \lambda_r^n \ ;\ \alpha_{j+1} \geq \alpha_j \geq \ldots \geq \alpha_{j+1-j_o} \ ;\ \sum_{n=j+1-j_o}^{j+1} \alpha_n = 1 \tag{3.42}$$

In addition, two constraints are considered in formulating the optimization problem:

(1) Barrier condition. According to the concept of dual-ring control, the timing period in ring A should be equal to the timing period in ring B on either side of the barrier, i.e.,

$$\begin{aligned}
G_1^{j+1} + G_2^{j+1} &= G_5^{j+1} + G_6^{j+1} \\
G_3^{j+1} + G_4^{j+1} &= G_7^{j+1} + G_8^{j+1}
\end{aligned} \tag{3.43}$$

(2) Equilibrium condition. The phase green is expected to be large enough to service all the vehicles that arrive during the effective red and effective green (plus initial queue) in order

to avoid oversaturation delay, i.e., to terminate the phase by gap-out control and invoke no vehicle spillover (refer to gap-out Case 1 and 2); therefore,

$$\begin{aligned} G_i^{j+1} &< G_{\max i}^{j+1} + L_i \\ G_{qi}^{j+1} &\le G_i^{j+1} - L_i \end{aligned} \tag{3.44}$$

where $\boldsymbol{G_{qi}^{j+1}} = \dfrac{\boldsymbol{Q_i^{j+1}(0)} + \boldsymbol{\lambda_i^{j+1}}\left(\boldsymbol{R_i^{j+1}} + \boldsymbol{L_i^{j+1}}\right)}{\boldsymbol{S_i} - \boldsymbol{\lambda_i^{j+1}}}$

Therefore, the complete optimization problem is expressed by

$$Min\left[\sum_{i=2,3,4,6,7,8} E\left(W_i^{j+1}\right) + \sum_{r=1,5} E\left(W_r^{j+2}\right)\right]$$

subject to

$$\begin{aligned} &G_1^{j+1} + G_2^{j+1} = G_5^{j+1} + G_6^{j+1} \\ &G_3^{j+1} + G_4^{j+1} = G_7^{j+1} + G_8^{j+1} \\ &G_{qi}^{j+1} + L_i \le G_i^{j+1} < G_{\max i}^{j+1} + L_i \end{aligned}$$

3.7 Determining optimal minimum green $G_{\min i}^{j+1}$

Minimum green is set equal to queue service time if queue service time is less than the pre-determined (i.e., traditional) minimum green, $G_{\min i}^{0}$, otherwise, set it equal to the pre-determined minimum green, i.e.,

$$\begin{aligned} G_{\min i}^{j+1} &= G_{qi}^{j+1} \quad \text{if} \quad G_{qi}^{j+1} \le G_{\min i}^{0} \\ G_{\min i}^{j+1} &= G_{\min i}^{0} \quad \text{if} \quad G_{qi}^{j+1} > G_{\min i}^{0} \end{aligned}$$

or,

$$G_{\min i}^{j+1} = \min\left[G_{qi}^{j+1}, G_{\min i}^{0}\right] \tag{3.45}$$

3.8 Determining optimal passage setting β_i^{j+1}

Recall that the optimized phase is expected to be terminated by gap-out control; therefore, the phase split can be expressed by Eq. (3.14), i.e.,

$$G_i^{j+1} = L_i + G_{\min i}^{j+1} + \frac{\exp\left(\lambda_i^{j+1}\beta_i^{j+1}\right) - 1}{\lambda_i^{j+1}}$$

Then,

$$\beta_i^{j+1} = \frac{\ln\left[1 + \lambda_i^{j+1}\left(G_i^{j+1} - G_{\min i}^{j+1} - L_i\right)\right]}{\lambda_i^{j+1}} \tag{3.46}$$

Note here that, the natural logarithm in Eq. (3.46) requires $\left[1 + \lambda_i^{j+1}\left(G_i^{j+1} - G_{\min i}^{j+1} - L_i\right)\right]$ be greater than zero. According to inequality (3.44), i.e.,

$$G_{qi}^{j+1} \le G_i^{j+1} - L_i$$

we have

$$G_{qi}^{j+1} - G_{\min i}^{j+1} \le G_i^{j+1} - L_i - G_{\min i}^{j+1} \tag{3.47}$$

And, according to Eq. (3.45), we have

$$\begin{aligned} &G_{qi}^{j+1} - G_{qi}^{j+1} \le G_i^{j+1} - L_i - G_{\min i}^{j+1} \quad \text{if } G_{qi}^{j+1} \le G_{\min i}^0 \\ &G_{qi}^{j+1} - G_{\min i}^0 \le G_i^{j+1} - L_i - G_{\min i}^{j+1} \quad \text{if } G_{qi}^{j+1} > G_{\min i}^0 \end{aligned}$$

or,

$$\begin{aligned} &0 \le G_i^{j+1} - L_i - G_{\min i}^{j+1} \quad \text{if } G_{qi}^{j+1} \le G_{\min i}^0 \\ &0 < G_i^{j+1} - L_i - G_{\min i}^{j+1} \quad \text{if } G_{qi}^{j+1} > G_{\min i}^0 \end{aligned}$$

Then,

$$\begin{aligned} &1 \le 1 + \lambda_i^{j+1}\left(G_i^{j+1} - L_i - G_{\min i}^{j+1}\right) \quad \text{if } G_{qi}^{j+1} \le G_{\min i}^0 \\ &1 < 1 + \lambda_i^{j+1}\left(G_i^{j+1} - L_i - G_{\min i}^{j+1}\right) \quad \text{if } G_{qi}^{j+1} > G_{\min i}^0 \end{aligned} \tag{3.48}$$

and the requirement imposed by the natural logarithm is satisfied. Substituting inequality (3.48) into Eq. (3.46), we have

$$\begin{aligned} &\beta_i^{j+1} \ge 0 \quad \text{if } G_{qi}^{j+1} \le G_{\min i}^0 \\ &\beta_i^{j+1} > 0 \quad \text{if } G_{qi}^{j+1} > G_{\min i}^0 \end{aligned} \tag{3.49}$$

4. Theoretical Development of Ramp Control Model

Assume Poisson arrivals at a ramp; i.e.,

$$P_i(t) = \frac{(\lambda t)^i e^{-\lambda t}}{i!} \tag{4.1}$$

Where the mean arrival rate $\bar{V}$ and variance σ^2 are given by

$$\bar{V} = \sigma^2 = \lambda t \tag{4.2}$$

The corresponding headway distribution is given by

$$\Pr(h \le t) = 1 - e^{-\lambda t} \tag{4.3}$$

Note that if the arrivals are formed by a sum of Poisson arrivals,

$$P_i^k(t) = \frac{m_k e^{-m_k}}{i!} \; ; \; m_k = \lambda_k t \; ; \; k = 1, \ldots, n \tag{4.4}$$

then,

$$P_i(t) = \frac{e^{-M} M^i}{i!} \;\; ; \;\; M = \sum_{k=1}^{n} m_k \; ; \; m_k = \lambda_k t \tag{4.5}$$

Note: The following derivation parallels that of Hokstad (1979).

Consider a stationary ramp queue. Let *X* denote the queue waiting time (not including the "service time" once the vehicle arrives at the ramp meter stop line). Let *Y* denote the "service time," which is simply the metering headway, or the inverse of the current ramp metering rate, M_R; initially, we assume that $\Pr(Y \le \alpha) = F(\alpha)$.

Assume that the ramp has a finite storage capacity, C_R (expressed in ft.). Then, it is assumed that, once the queue length reaches this limit, any further ramp-bound vehicles will be diverted. This condition is specified by

$$X + Y \begin{cases} < K \Rightarrow \text{vehicle will join the ramp queue} \\ \ge K \Rightarrow \text{vehicle will be diverted and not join the ramp queue} \end{cases} \tag{4.6}$$

where

$$K = \frac{C_R \cdot Y}{L_V} \;\; ; \;\; L_V = \text{ Average length of a vehicle} \tag{4.7}$$

Therefore, $X \le K$.

Following Takacs (1955), let $\eta(t)$ denote the waiting time at the ramp at time instant *t*. Denote $\eta(0) = \eta_0$ with distribution function $\Pr(\eta_0 \le x) = W_0^*(x)$. Let $\Pr(\eta(t) \le x) = W^*(t, x)$.

Consider $W^*(t + \Delta t, x)$. The event $\eta(t + \Delta t) \le x$ can occur in the following mutually exclusive, and exhaustive, ways:

1. During the interval $(t, t + \Delta t)$ no event occurs; the probability of this outcome is $1 - \lambda\Delta t + o(\Delta t)$. Then , for this outcome, $\Pr[\eta(t) \le x + \Delta t] = W^*(t, x + \Delta t)$.

2. During the interval $(t, t + \Delta t)$ one event occurs—the probability of this outcome is $\lambda\Delta t + o(\Delta t)$—and the waiting time $\eta(t) = y$, where $0 \le y \le x$. For this, we must have $Y \le x - y$, which occurs with probability:

$$\int_0^x F(x-u)\, d_u W^*(t,u) \tag{4.8}$$

   Then , for this outcome,

$$\begin{aligned} \Pr[\eta(t) \le x + \Delta t] &= [\lambda\Delta t + o(\Delta t)] \int_0^x F(x-u)\, d_u W^*(t,u) \\ &= \lambda\Delta t \int_0^x F(x-u)\, d_u W^*(t,u) + o(\Delta t) \end{aligned} \tag{4.9}$$

3. During the interval $(t, t + \Delta t)$ more than one event occurs; the probability of this outcome is $o(\Delta t)$.

Then,

$$W^*(t + \Delta t, x) = (1 - \lambda\Delta t) W^*(t, x + \Delta t) + \lambda\Delta t \int_0^x F(x-u)\, d_u W^*(t,u) + o(\Delta t) \tag{4.10}$$

But,

$$W^*(t, x + \Delta t) = W^*(t, x) + \frac{\partial W^*(t,x)}{\partial x}\Delta t + o(\Delta t) \tag{4.11}$$

So,

$$W^*(t+\Delta t,x)=(1-\lambda\Delta t)\left[W^*(t,x)+\frac{\partial W^*(t,x)}{\partial x}\Delta t\right]+\lambda\Delta t\int_0^x F(x-u)d_uW^*(t,u)+o(\Delta t)$$
$$=W^*(t,x)+\frac{\partial W^*(t,x)}{\partial x}\Delta t-\lambda\Delta t\cdot W^*(t,x)+\lambda\Delta t\int_0^x F(x-u)d_uW^*(t,u)+o(\Delta t) \quad (4.12)$$

Or,

$$\frac{W^*(t+\Delta t,x)-W^*(t,x)}{\Delta t}=\frac{\partial W^*(t,x)}{\partial x}-\lambda\cdot W^*(t,x)+\lambda\int_0^x F(x-u)d_uW^*(t,u)+o(\Delta t) \quad (4.13)$$

Taking the limit as $\Delta t\to 0$,

$$\frac{\partial W^*(t,x)}{\partial t}=\frac{\partial W^*(t,x)}{\partial x}-\lambda\cdot W^*(t,x)+\lambda\int_0^x F(x-u)d_uW^*(t,u) \quad (4.14)$$

Consider stationary solutions, i.e., solutions satisfying

$$\frac{\partial W^*(t,x)}{\partial t}=0\Rightarrow W^*(t,x)=W(x) \quad (4.15)$$

where we define

$$W(x)=\lim_{t\to\infty}W^*(t,x)=\Pr(X\le x)$$
$$Q=\Pr(X=0)=W(0) \quad (4.16)$$

We note that, from the condition $X\le K$, $W(K)=1$. Then, $w(x)=dW(x)/dx$ exists for all $x>0$, and is defined by the integral-differential equation

$$w(x)=\frac{dW(x)}{\partial x}=\lambda\cdot W(x)-\lambda\int_0^x F(x-u)dW(u) \quad (4.17)$$

The probability that the waiting time will be between u and $u+\delta u$ is simply $dW(u)$ times the probability that the vehicle will join the queue; this latter probability is simply the probability that the service time Y is $\le K-u$, or $F(K-u)$. (Recall $W(K)\equiv 1$.) Then,

$$W(x)=\int_0^x F(K-u)dW(u) \quad (4.18)$$

and

$$
\begin{aligned}
w(x) &= \lambda \int_0^x F(K-u)\,dW(u) - \lambda \int_0^x F(x-u)\,dW(u) \\
&= \lambda \int_0^x \left[F(K-u) - F(x-u) \right] dW(u) \;;\; 0 \le x \le K
\end{aligned}
\tag{4.19}
$$

We assume that the "service times" are independent with cumulative distribution function (cdf) $F(y) = \Pr(Y \le y)$. In the case where the "service times" can be assumed to be equal to the metering headway, $b = M_R^{-1}$,

$$
F(y) = \Pr(Y \le y) = \begin{cases} 1, & y \ge b \\ 0, & y < b \end{cases} = H(b) \tag{4.20}
$$

where $H(\cdot)$ is the Heaviside step function.

Let *n* be an integer satisfying

$$nb \le K < (n+1)b \;;\; n = 1, 2, \ldots$$

(Note: we exclude the case $n = 0$ since it corresponds to the case in which no vehicle is allowed to enter the system; we also treat the case $n = 1$ separately.) Assume $n \ge 2$. Divide the interval $[0, K]$ into $n+2$ subintervals; i.e.,

$$
\begin{aligned}
I_k &= \{ x : kb \le x < (k+1)b \}; \quad k = 0, 1, 2, \ldots, n-2 \\
I_{n-1} &= \{ x : (n-1)b \le x < K - b \} \\
I_n &= \{ x : K - b \le x < nb \} \\
I_{n+1} &= \{ x : nb \le x < K \}
\end{aligned}
\tag{4.21}
$$

Let

$$
\begin{aligned}
W_k(x) &= W(x) \;;\; x \in I_k,\; k = 0, 1, \ldots, n+1 \\
w_k(x) &= w(x) \;;\; x \in I_k,\; k = 0, 1, \ldots, n+1
\end{aligned}
\tag{4.22}
$$

Then

$$
\begin{aligned}
w(x) &= \lambda \int_0^x \left[F(K-u) - F(x-u) \right] dW(u) \;;\; 0 < x \le K \\
&= \lambda \int_0^x dW(u) \; - \lambda \int_0^x F(x-u)\,dW(u) \;;\; 0 < x \le K
\end{aligned}
\tag{4.23}
$$

$$
w_0(x) = \lambda W_0(x) \tag{4.24a}
$$

$$w_k(x) = \lambda\left[\int_0^b dW_0(u) + \int_b^{2b} dW_1(u) + \ldots + \int_{(k-1)b}^{kb} dW_{k-1}(u) + \int_{kb}^{x} dW_k(u)\right]$$
$$-\lambda\left[\int_0^b dW_0(u) + \int_b^{2b} dW_1(u) + \ldots + \int_{(k-1)b}^{x-b} dW_{k-1}(u)\right]$$
$$= \lambda\left[\int_{(k-1)b}^{kb} dW_{k-1}(u) + \int_{kb}^{x} dW_k(u) - \int_{(k-1)b}^{x-b} dW_{k-1}(u)\right] \qquad (4.24b)$$
$$= \lambda\left[W_{k-1}(kb) - W_{k-1}\big((k-1)b\big) + W_k(x) - W_k(kb) - W_{k-1}(x-b) + W_{k-1}\big((k-1)b\big)\right]$$
$$= \lambda\left[W_{k-1}(kb) + W_k(x) - W_k(kb) - W_{k-1}(x-b)\right];\ \text{Note: } W_{k-1}(kb) = W_k(kb)$$
$$= \lambda\left[W_k(x) - W_{k-1}(x-b)\right]\ ;\ \ k = 1, 2, \ \ldots\ , n-1$$

$$w_n(x) = \lambda\left[W_{n-1}(K-b) - W_{n-2}(x-b)\right] \qquad (4.24c)$$

$$w_{n+1}(x) = \lambda\left[W_{n-1}(K-b) - W_{n-1}(x-b)\right] \qquad (4.24d)$$

$$w_0(x) = \lambda\int_0^x \left[F(K-u) - F(x-u)\right] dW(u)\ ;\ \ 0 \le x < b$$
$$= \lambda\int_0^x F(\overset{\nearrow 1}{K-u})\, dW(u) - \lambda\int_0^x F(\overset{\nearrow 0}{x-u})\, dW(u)\ ;\ \ 0 \le x < b$$
$$= \lambda\int_0^x dW(u)\ ;\ \ 0 \le x < b$$
$$= \lambda W_0(x)$$

$$w_0(x) = \frac{dW_0(x)}{dx} = \lambda W_0(x) \Rightarrow\ W_0(x) = ce^{\lambda x}$$

But,

$$W_0(0) = Q = ce^{\lambda 0}\ \Rightarrow\ c = Q$$

So,

$$W_0(x) = Qe^{\lambda x} \qquad (4.25a)$$

$$w_1(x) = \frac{dW_1(x)}{dx} = \lambda\left[W_1(x) - W_0(x-b)\right]$$
$$= \lambda\left[W_1(x) - Qe^{\lambda(x-b)}\right]$$

$$\frac{dW_1(x)}{dx} - \lambda W_1(x) = -\lambda Q e^{\lambda(x-b)}$$
$$W_1(x) = Qe^{\lambda x}\left[1 - \lambda e^{-\lambda b}(x-b)\right]$$

$$w_2(x) = \frac{dW_2(x)}{dx} = \lambda\left[W_2(x) - W_1(x-b)\right]$$
$$= \lambda\left\{W_2(x) - Qe^{\lambda(x-b)}\left[1 - \lambda e^{-\lambda b}(x-2b)\right]\right\}$$

$$\frac{dW_2(x)}{dx} - \lambda W_2(x) = -Qe^{\lambda(x-b)}\left[1 - \lambda e^{-\lambda b}(x-2b)\right]$$
$$W_2(x) = Qe^{\lambda x}\left[1 - \lambda e^{-\lambda b}(x-b) + \frac{\lambda^2}{2}e^{-2\lambda b}(x-2b)^2\right]$$

In general,

$$W_k(x) = Qe^{\lambda x}\sum_{j=0}^{k}\frac{(-\lambda)^j}{j!}e^{-j\lambda b}(x-jb)^j \quad ; \quad k = 0,1,\ldots,n-1 \tag{4.25b}$$

And, from (4.24c) and (4.24d),

$$\frac{dW_n(x)}{dx} = \lambda\left[W_{n-1}(K-b) - W_{n-2}(x-b)\right]$$

$$W_n(x) = \lambda(x-K+B)W_{n-1}(x) + \sum_{k=0}^{n-1}W_k\left[K-(n-k)b\right] - \sum_{k=0}^{n-2}W_k\left[x-(n-1-k)b\right] \tag{4.25c}$$

$$\frac{dW_{n+1}(x)}{dx} = \lambda\left[W_{n-1}(K-b) - W_{n-1}(x-b)\right]$$

$$W_{n+1}(x) = Q + \lambda(x-K+b)W_{n-1}(K-b) + \sum_{k=0}^{n-1}\left[W_k\left(K-(n-k)b\right) - W_k\left(x-(n-k)b\right)\right] \tag{4.25d}$$

Observe that, from (4.25d),

$$W_{n+1}(K) = Q + \lambda b W_{n-1}(K-b) \tag{4.26}$$

And, from the condition $X \le K$, $W(K) = 1$. So,

$$Q + \lambda b W_{n-1}(K-b) = 1 \tag{4.27}$$

Evaluating (4.25b) for $k = n-1$, we get

$$W_{n-1}(x) = Qe^{\lambda x}\sum_{j=0}^{n-1}\frac{(-\lambda)^j}{j!}e^{-j\lambda b}(x-jb)^j$$
$$W_{n-1}(K-b) = Qe^{\lambda(K-b)}\sum_{j=0}^{n-1}\frac{(-\lambda)^j}{j!}e^{-j\lambda b}\left(K-(j+1)b\right)^j \quad (4.28)$$

Substituting (4.28) into (4.27)

$$Q+\lambda b\left\{Qe^{\lambda(K-b)}\sum_{j=0}^{n-1}\frac{(-\lambda)^j}{j!}e^{-j\lambda b}\left(K-(j+1)b\right)^j\right\}=1$$

From which,

$$Q\left[1+\lambda be^{\lambda(K-b)}\sum_{j=0}^{n-1}\frac{(-\lambda)^j}{j!}e^{-j\lambda b}\left(K-(j+1)b\right)^j\right]=1$$
$$Q=\left[1+\lambda be^{\lambda(K-b)}\sum_{j=0}^{n-1}\frac{(-\lambda)^j}{j!}e^{-j\lambda b}\left(K-(j+1)b\right)^j\right]^{-1} \quad (4.29)$$

Recall, from (4.16), i.e.,

$$W(x)=\lim_{t\to\infty}W^*(t,x)=\Pr(X\le x)$$
$$Q=\Pr(X=0)=W(0) \quad (4.16)$$

So, the cumulative distribution function for X, the queue waiting time, under the conditions of Poisson arrivals with mean arrival rate λ, and metering headway $b=M_R^{-1}$, and finite storage capacity, $C_R=K\cdot L_V/b$, is given by:

$$\Pr(x=0)=W(0)=\left[1+\lambda be^{\lambda(K-b)}\sum_{j=0}^{n-1}\frac{(-\lambda)^j}{j!}e^{-j\lambda b}\left(K-(j+1)b\right)^j\right]^{-1}$$

$$\Pr(X\le x)=W_0(x)=Qe^{\lambda x}\ ;\ \{0\le x<b\}$$

$$\Pr(X\le x)=W_k(x)=Qe^{\lambda x}\sum_{j=0}^{k}\frac{(-\lambda)^j}{j!}e^{-j\lambda b}(x-jb)^j\ ;\ k=1,2,\ \ldots,n-1;\ \{kb\le x<(k+1)b\}$$

$$\Pr(X\le x)=W_n(x)=\lambda(x-K+b)W_{n-1}(x)+\sum_{k=0}^{n-1}W_k\left[K-(n-k)b\right]-\sum_{k=0}^{n-2}W_k\left[x-(n-1-k)b\right];\ \{K-b\le x<nb\}$$

$$\Pr(X \le x) = W_{n+1}(x) = Q + \lambda(x - K + b)W_{n-1}(K - b) + \sum_{k=0}^{n-1}\left[W_k\left(K - (n-k)b\right) - W_k\left(x - (n-k)b\right)\right] \; ; \; \{nb \le x < K\}$$

Observe that the probability that a random arrival J joins the system is given by

$$\Pr(J) = \Pr\left(\text{Arbitrary arrival enters ramp system}\right) = W_{n-1}(K - b) \tag{4.30}$$

Or, from (4.27),

$$\Pr(J) = \frac{1 - Q}{\lambda b} \tag{4.31}$$

Let M denote the number of vehicles queued on the ramp. Then,

$$\Pr(M \le m) = \Pr(X \le mb) = W_m(mb) \; ; \; m = 0,1, \ldots, n-1 \tag{4.32a}$$

$$\Pr(M \le n) = W_n(nb) = \lambda\left((n+1)b - K\right)W_{n-1}(K - b) + \sum_{k=0}^{n-1} W_k\left[K - (n-k)b\right] - \sum_{k=0}^{n-2} W_k\left[(k+1)b\right] \tag{4.32b}$$

The mean queue length is simply

$$E(M) = \sum_{m=0}^{n} \Pr(M > m) \tag{4.33}$$

Or,

$$
\begin{aligned}
E(M) &= \sum_{m=0}^{n}\left[1-\Pr(M \le m)\right] \\
&= n+1-\sum_{m=0}^{n}\Pr(M \le m) \\
&= n+1-\Pr(M \le n)-\sum_{m=0}^{n-1}W_m(mb) \\
&= n+1-\left\{\lambda\left((n+1)b-K\right)W_{n-1}(K-b)+\sum_{k=0}^{n-1}W_k\left[K-(n-k)b\right]-\sum_{k=0}^{n-2}W_k\left[(k+1)b\right]\right\}-\sum_{m=0}^{n-1}W_m(mb) \\
&= n+1-\lambda\left((n+1)b-K\right)W_{n-1}(K-b)-\sum_{k=0}^{n-1}W_k\left[K-(n-k)b\right]+\sum_{k=0}^{n-2}W_k\left[(k+1)b\right]-\sum_{m=0}^{n-1}W_m(mb) \\
&= n+1-\lambda\left((n+1)b-K\right)W_{n-1}(K-b)-\sum_{k=0}^{n-1}W_k\left[K-(n-k)b\right]+\sum_{k=0}^{n-2}W_k\left[(k+1)b\right]-\sum_{m=1}^{n-1}W_m(mb)-W_0(0) \\
&= n+1-\lambda\left((n+1)b-K\right)W_{n-1}(K-b)-\sum_{k=0}^{n-1}W_k\left[K-(n-k)b\right]+\sum_{k=0}^{n-2}W_k\left[(k+1)b\right]-\sum_{k=0}^{n-2}W_{k+1}\left[(k+1)b\right]-W_0(0)
\end{aligned}
$$

But,

$$W_k\left[(k+1)b\right] = W_{k+1}\left[(k+1)b\right] \;;\; k = 0,1,\ \ldots, n-2$$

So,

$$E(M) = n+1-\lambda\left((n+1)b-K\right)W_{n-1}(K-b)-\sum_{k=0}^{n-1}W_k\left[K-(n-k)b\right]-W_0(0)$$

But, $W_0(0) \equiv Q$ and, from (4.17), $Q+\lambda b W_{n-1}(K-b)=1$. So,

$$E(M) = n+1-\lambda\left((n+1)b-K\right)W_{n-1}(K-b)-\sum_{k=0}^{n-1}W_k\left[K-(n-k)b\right]-1+\lambda b W_{n-1}(K-b)$$

Or,

$$E(M) = n+\lambda\left(K-nb\right)W_{n-1}(K-b)-\sum_{k=0}^{n-1}W_k\left[K-(n-k)b\right] \qquad (4.34)$$

Using Little's formula, see e.g., Kleinrock (1975), the expected number of vehicles on the ramp, $E(M_q)$, is given by

$$E(M_q) = E(M)-(1-Q) \qquad (4.35)$$

The arrival rate of those vehicles that actually enter the ramp is given by

$$\lambda_R = \lambda \Pr(J) \tag{4.36}$$

But, from (4.31), i.e.,

$$\Pr(J) = \frac{1-Q}{\lambda b} \tag{4.31}$$

So,

$$\lambda_R = \frac{1-Q}{b} \tag{4.37}$$

Little's formula gives

$$E(M_q) = \lambda_R E(X) \tag{4.38}$$

Then, the mean waiting time can be computed as

$$\begin{aligned} E(X) &= \frac{E(M_q)}{\lambda_R} = \frac{E(M)-(1-Q)}{(1-Q)} b = \left[\frac{E(M)}{(1-Q)} - 1 \right] b \\ &= \left[\frac{n + \lambda\left(K - nb\right) W_{n-1}(K-b) - \sum_{k=0}^{n-1} W_k \left[K - (n-k)b\right]}{(1-Q)} - 1 \right] b \end{aligned} \tag{4.39}$$

where

$$W_0(x) = Qe^{\lambda x}$$

$$W_k(x) = Qe^{\lambda x} \sum_{j=0}^{k} \frac{(-\lambda)^j}{j!} e^{-j\lambda b} (x - jb)^j \quad ; \quad k = 0,1, \ldots, n-1$$

$$Q = \left[1 + \lambda b e^{\lambda(K-b)} \sum_{j=0}^{n-1} \frac{(-\lambda)^j}{j!} e^{-j\lambda b} \left(K - (j+1)b\right)^j \right]^{-1}$$

5. Consideration of Freeway Delay

As discussed in Section 2, the flow–density picture presented by actual field data suggests an underlying theoretical model of the form first proposed by Gordon Newell (of UC Berkeley), known as the "triangular" flow – density relationship, it has the mathematical form:

$$q = \begin{cases} S_f \cdot k \;\; ; \;\; k \le k_c \\ q_c \cdot \left(1 - \dfrac{k - k_c}{k_j - k_c} \right) \;\; ; \;\; k_j \le k \le k_c \end{cases} \tag{2.1}$$

$$\dot{x} = \begin{cases} S_f \;\; ; \;\; k \le k_c \\ \dfrac{S_f}{\dfrac{k_j}{k_c} - 1} \cdot \left(\dfrac{k_j}{k} - 1 \right) \;\; ; \;\; k_j \le k \le k_c \end{cases} \tag{2.2}$$

Here, we adopt this model to represent the freeway component of the corridor system. A feature of this representation is that the freeway speed remains relatively constant for densities below the critical density, k_c; thus, there is no appreciable freeway delay for values $k \le k_c$. We note also that

$$k = \frac{q}{S_f} \;\; ; k \le k_c \tag{5.1}$$

Downstream of a ramp entry point, provided that densities are restricted to be $\le k_c$,

$$k = \frac{q_u + M_R}{S_f} \;\; ; k \le k_c \tag{5.2}$$

where q_u is the mainline flow rate immediately upstream of the ramp. Or,

$$k = k_u + \frac{M_R}{S_f} \;\; ; k \le k_c \tag{5.3}$$

Enforcing such conditions will result in (approximately) zero delay to the freeway. In the optimal control formulation based on minimizing total delay (as well as any combination of component delays), this condition places the following constraint on the solution:

$$k_u + \frac{M_R}{S_f} \le k_c \tag{5.4}$$

6. Development of Integrated Control Model

The integrated control of the combined intersection and ramp system can be formulated as a nonlinear, multi-objective, programming problem. Consider some intersection *k* that provides

access to freeway entry ramp R. Let δ_{ik}^{R} denote the proportion of traffic associated with NEMA phase i at intersection k that contribute flow to ramp R; specifically, $\delta_{ik}^{R} \equiv 0$ for phases that do not feed the ramp, $\delta_{ik}^{R} \equiv 1$ for phases that exclusively feed the ramp, and $0 \le \delta_{ik}^{R} \le 1$ for phases in which it is optional to feed the ramp. Then, during any particular cycle of operation of length C, the ramp arrival rate, λ, is determined by

$$\lambda = \sum_{\forall \text{ NEMA } i} \delta_{ik}^{R} q_{ik}^{j} \tag{6.1}$$

where q_{ik}^{j} are determined via the procedure outlined in Section 3.4 above; i.e., from (3.27)

$$E(q_{ik}^{j'}) = N(G_{ik}^{j'}) / C_{k}^{j'} \tag{3.27}$$

where

$$C_{k}^{j'} = \sum_{i=1}^{4} G_{ik}^{j'}$$

Then, from (4.39) above and noting that $b = M_R^{-1}$, the mean waiting time can be computed as

$$\begin{aligned} E(X) &= \frac{E(M_q)}{\lambda_R} = \frac{E(M) - (1-Q)}{(1-Q)} b = \left[\frac{E(M)}{(1-Q)} - 1 \right] M_R^{-1} \\ &= \left[\frac{n + \lambda\left(K - nM_R^{-1}\right) W_{n-1}(K - M_R^{-1}) - \sum_{k=0}^{n-1} W_k \left[K - (n-k) M_R^{-1} \right]}{(1-Q)} - 1 \right] M_R^{-1} \end{aligned} \tag{6.2}$$

where

$$W_0(x) = Qe^{\lambda x}$$

$$W_k(x) = Qe^{\lambda x} \sum_{j=0}^{k} \frac{(-\lambda)^j}{j!} e^{-j\lambda M_R^{-1}} (x - jM_R^{-1})^j \quad ; \quad k = 0,1, \ldots, n-1$$

$$Q = \left[1 + \lambda M_R^{-1} e^{\lambda (K - M_R^{-1})} \sum_{j=0}^{n-1} \frac{(-\lambda)^j}{j!} e^{-j\lambda M_R^{-1}} \left(K - (j+1) M_R^{-1} \right)^j \right]^{-1}$$

And, from (4.37) and (4.38) above, i.e.,

$$\lambda_R = \frac{1-Q}{b} = (1-Q) M_R \tag{4.37}$$

$$E(M_q) = \lambda_R E(X) \tag{4.38}$$

the total expected delay due to ramp metering is

$$\begin{aligned} D_R &= E(M_q)E(X) \\ &= \lambda_R E(X)^2 \end{aligned} \tag{6.3}$$

Substituting (6.2) and (4.37),

$$D_R = (1-Q)\left[\frac{n+\lambda\left(K-nM_R^{-1}\right)W_{n-1}(K-M_R^{-1}) - \sum_{k=0}^{n-1} W_k\left[K-(n-k)M_R^{-1}\right]}{(1-Q)} - 1\right]^2 M_R^{-1} \tag{6.4}$$

So, the problem of minimizing the ramp delay can be stated as:

$$\underset{M_R,\lambda}{Min}\, D_R = (1-Q)\left[\frac{n+\lambda\left(K-nM_R^{-1}\right)W_{n-1}(K-M_R^{-1}) - \sum_{k=0}^{n-1} W_k\left[K-(n-k)M_R^{-1}\right]}{(1-Q)} - 1\right]^2 M_R^{-1} \tag{6.5}$$

subject to:

$$\lambda = \sum_{\forall \text{ NEMA } i} \delta_{ik}^R q_{ik}^j \tag{6.5a}$$

$$W_0(x) = Qe^{\lambda x} \tag{6.5b}$$

$$W_k(x) = Qe^{\lambda x}\sum_{j=0}^{k}\frac{(-\lambda)^j}{j!}e^{-j\lambda b}(x-jM_R^{-1})^j \;\; ; \;\; k = 0,1,\ldots,n-1 \tag{6.5c}$$

$$Q = \left[1+\lambda M_R^{-1}e^{\lambda(K-M_R^{-1})}\sum_{j=0}^{n-1}\frac{(-\lambda)^j}{j!}e^{-j\lambda M_R^{-1}}\left(K-(j+1)M_R^{-1}\right)^j\right]^{-1} \tag{6.5d}$$

$$k_u + \frac{M_R}{S_f} \le k_c \tag{6.5e}$$

$$M_R^{Min} \le M_R \le M_R^{Max} \tag{6.5f}$$

$$M_R, \lambda \ge 0 \tag{6.5g}$$

Recall that the problem of minimizing signal delay, D_S, is given by (3.41) above, i.e.,

$$Min\left[\sum_{i=2,3,4,6,7,8} E\left(W_i^{j+1}\right)+\sum_{r=1,5} E\left(W_r^{j+2}\right)\right]$$

subject to

$$E\left(W_i^{j+1}\right)=\frac{S_i\lambda_i^{j+1}}{2(S_i-\lambda_i^{j+1})}\left\{(R_i^{j+1})^2+R_i^{j+1}\left(\frac{2}{\lambda_i^{j+1}}Q_i^{j+1}(0)+\frac{1}{S_i}+\frac{1}{S_i-\lambda_i^{j+1}}\right)\right\}$$

$$E\left(W_r^{j+2}\right)=\frac{S_r\lambda_r^{j+2}}{2(S_r-\lambda_r^{j+2})}\left\{(R_r^{j+2})^2+R_r^{j+2}\left(\frac{2}{\lambda_r^{j+2}}Q_r^{j+2}(0)+\frac{1}{S_r}+\frac{1}{S_r-\lambda_r^{j+2}}\right)\right\}$$

$$R_1^{j+2}=G_2^{j+1}+G_3^{j+1}+G_4^{j+1}$$

$$R_2^{j+1}=G_3^{j}+G_4^{j}+G_1^{j+1}$$

$$R_3^{j+1}=G_4^{j}+G_1^{j+1}+G_2^{j}$$

$$R_4^{j+1}=G_1^{j+1}+G_2^{j+1}+G_3^{j+1}$$

$$R_5^{j+2}=G_6^{j+1}+G_7^{j+1}+G_8^{j+1}$$

$$R_6^{j+1}=G_7^{j}+G_8^{j}+G_5^{j+1}$$

$$R_7^{j+1}=G_8^{j}+G_5^{j+1}+G_6^{j+1}$$

$$R_8^{j+1}=G_5^{j+1}+G_6^{j+1}+G_7^{j+1}$$

$$G_1^{j+1}+G_2^{j+1}=G_5^{j+1}+G_6^{j+1}$$

$$G_3^{j+1}+G_4^{j+1}=G_7^{j+1}+G_8^{j+1}$$

$$G_{qi}^{j+1}+L_i\le G_i^{j+1}<G_{\max i}^{j+1}+L_i$$

$$\boldsymbol{G_{qi}^{j+1}=\frac{Q_i^{j+1}(0)+\lambda_i^{j+1}\left(R_i^{j+1}+L_i^{j+1}\right)}{S_i-\lambda_i^{j+1}}}$$

In a multi-objective formulation, the ramp and signal delays (for intersections feeding freeway entry ramps) form a two-element set:

$$\mathbf{D}=\left\{\left[\sum_{i=2,3,4,6,7,8} E\left(W_i^{j+1}\right)+\sum_{r=1,5} E\left(W_r^{j+2}\right)\right],(1-Q)\left[\frac{n+\lambda\left(K-nM_R^{-1}\right)W_{n-1}(K-M_R^{-1})-\sum_{k=0}^{n-1}W_k\left[K-(n-k)M_R^{-1}\right]}{(1-Q)}-1\right]^2 M_R^{-1}\right\} \qquad (6.6)$$

and the multi-objective problem can be stated as:

$$Min\ \mathbf{D}=\left\{\left[\sum_{i=2,3,4,6,7,8} E\left(W_i^{j+1}\right)+\sum_{r=1,5} E\left(W_r^{j+2}\right)\right],(1-Q)\left[\frac{n+\lambda\left(K-nM_R^{-1}\right)W_{n-1}(K-M_R^{-1})-\sum_{k=0}^{n-1}W_k\left[K-(n-k)M_R^{-1}\right]}{(1-Q)}-1\right]^2 M_R^{-1}\right\} \qquad (6.7)$$

subject to:

$$E\left(W_i^{j+1}\right) = \frac{S_i \lambda_i^{j+1}}{2(S_i - \lambda_i^{j+1})}\left\{(R_i^{j+1})^2 + R_i^{j+1}\left(\frac{2}{\lambda_i^{j+1}}Q_i^{j+1}(0) + \frac{1}{S_i} + \frac{1}{S_i - \lambda_i^{j+1}}\right)\right\} \tag{6.8}$$

$$E\left(W_r^{j+2}\right) = \frac{S_r \lambda_r^{j+2}}{2(S_r - \lambda_r^{j+2})}\left\{(R_r^{j+2})^2 + R_r^{j+2}\left(\frac{2}{\lambda_r^{j+2}}Q_r^{j+2}(0) + \frac{1}{S_r} + \frac{1}{S_r - \lambda_r^{j+2}}\right)\right\} \tag{6.8b}$$

$$\begin{aligned}
&R_1^{j+2} = G_2^{j+1} + G_3^{j+1} + G_4^{j+1} \\
&R_2^{j+1} = G_3^{j} + G_4^{j} + G_1^{j+1} \\
&R_3^{j+1} = G_4^{j} + G_1^{j+1} + G_2^{j} \\
&R_4^{j+1} = G_1^{j+1} + G_2^{j+1} + G_3^{j+1} \\
&R_5^{j+2} = G_6^{j+1} + G_7^{j+1} + G_8^{j+1} \\
&R_6^{j+1} = G_7^{j} + G_8^{j} + G_5^{j+1} \\
&R_7^{j+1} = G_8^{j} + G_5^{j+1} + G_6^{j+1} \\
&R_8^{j+1} = G_5^{j+1} + G_6^{j+1} + G_7^{j+1} \\
&G_1^{j+1} + G_2^{j+1} = G_5^{j+1} + G_6^{j+1} \\
&G_3^{j+1} + G_4^{j+1} = G_7^{j+1} + G_8^{j+1} \\
&G_{qi}^{j+1} + L_i \le G_i^{j+1} < G_{\max i}^{j+1} + L_i
\end{aligned} \tag{6.8c}$$

$$\boldsymbol{G_{qi}^{j+1}} = \frac{\boldsymbol{Q_i^{j+1}}(0) + \boldsymbol{\lambda_i^{j+1}}\left(\boldsymbol{R_i^{j+1}} + \boldsymbol{L_i^{j+1}}\right)}{\boldsymbol{S_i} - \boldsymbol{\lambda_i^{j+1}}} \tag{6.8d}$$

$$\lambda = \sum_{\forall \text{ NEMA } i} \delta_{ik}^R q_{ik}^j \tag{6.8e}$$

$$\hat{W}_0(x) = Qe^{\lambda x} \tag{6.8f}$$

$$\hat{W}_k(x) = Qe^{\lambda x}\sum_{j=0}^{k}\frac{(-\lambda)^j}{j!}e^{-j\lambda b}(x - jM_R^{-1})^j \;\; ; \;\; k = 0,1,\ldots,n-1 \tag{6.8g}$$

$$Q = \left[1 + \lambda M_R^{-1} e^{\lambda(K - M_R^{-1})}\sum_{j=0}^{n-1}\frac{(-\lambda)^j}{j!}e^{-j\lambda M_R^{-1}}\left(K - (j+1)M_R^{-1}\right)^j\right]^{-1} \tag{6.8h}$$

$$k_u + \frac{M_R}{S_f} \le k_c \tag{6.8i}$$

$$M_R^{Min} \le M_R \le M_R^{Max} \tag{6.8j}$$

For the special case in which we wish to minimize total delay, D_T, which is simply the sum of the ramp and signal delay (for intersections feeding freeway entry ramps), i.e.,

$$D_T = D_S + D_R \tag{6.9}$$

the problem can be stated as:

$$Min\left\{\left[\sum_{i=2,3,4,6,7,8} E\left(W_i^{j+1}\right) + \sum_{r=1,5} E\left(W_r^{j+2}\right)\right] + \left(1-Q\right)\left[\frac{n+\lambda\left(K-nM_R^{-1}\right)W_{n-1}(K-M_R^{-1}) - \sum_{k=0}^{n-1} W_k\left[K-(n-k)M_R^{-1}\right]}{(1-Q)} - 1\right]^2 M_R^{-1}\right\} \tag{6.10}$$

subject to the conditions imposed by (6.8).

7. Simulation Evaluation

7.1 Simulation model setup

The proposed control strategies are tested and evaluated using a scalable, high-performance microscopic simulation package, Paramics (Cameron, G.D.B. and Duncan, G.I.B., 1996). Paramics has been widely used in the testing of various algorithms and evaluation of various Intelligent Transportation System (ITS) strategies because of its powerful Application Programming Interfaces (API), through which users can access the core models to customize and extend many features of the underlying simulation model, without having to deal with the underlying proprietary source codes. The proposed adaptive control model is implemented as a Paramics plug-in through API programming. It is noted that, although the theoretical models for adaptive control are developed under the assumption of Poisson arrivals (in order to obtain tractable mathematical results), in the simulation the arrival patterns are determined by the microsimulation and are, in general, not Poisson (particularly for peak flow conditions). As a result, the models themselves may represent only a crude approximation to actual conditions; it can be expected that, relaxing the assumption of Poisson arrivals (to the extent that such is possible) would produce improved results.

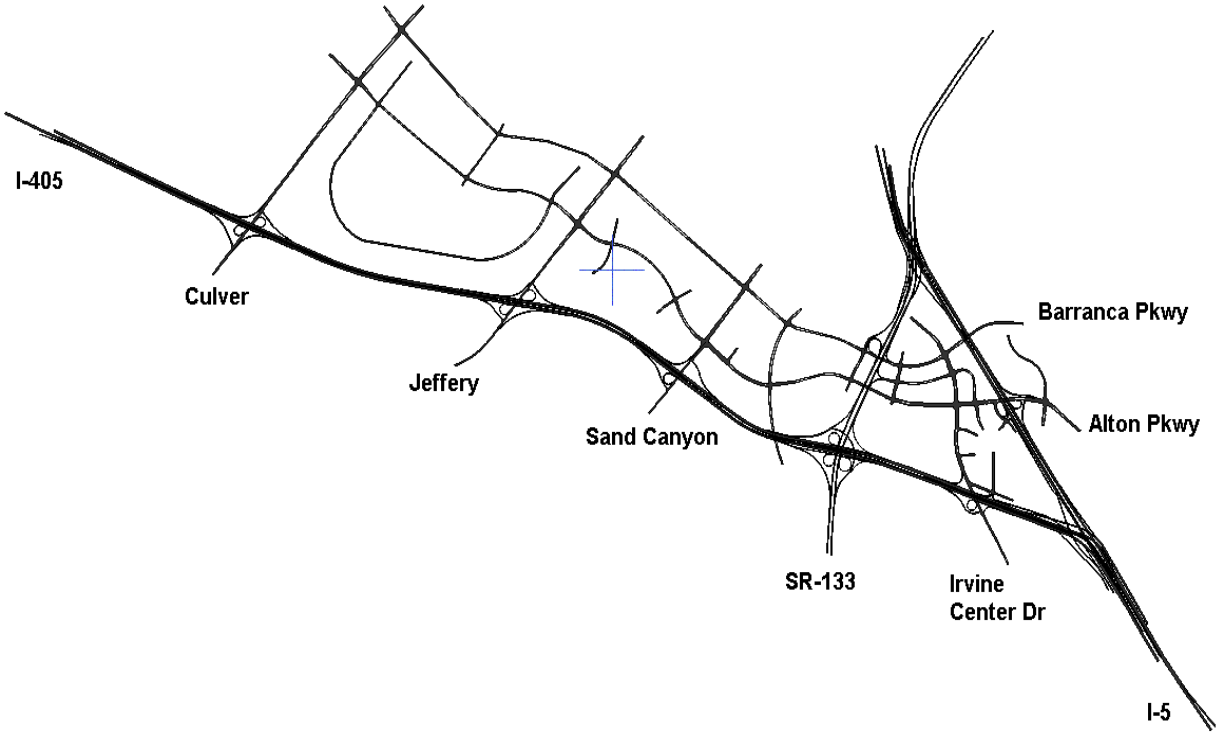

Figure 19. Test Network

The study network is shown as in Figure 19, which is so-called the "Irvine Triangle" located in southern California. A previous study calibrated this network in Paramics for the morning peak period from 6 to 10 AM (Chu, L. et al., 2004). This network includes a 6-mile section of freeway I-405, a 3-mile section of freeway I-5, a 3-mile section of freeway SR-133 and several adjacent surface streets, including two streets parallel to I-405 (i.e. Alton Parkway and Barranca Parkway), one street parallel to I-5 (Irvine Center Drive), and three crossing streets to I-405 (i.e. Culver Drive, Jeffery Road, and Sand Canyon Avenue). A total of thirty-eight signals under free-mode actuated control are included in this network.

Three traffic demand scenarios are set up to test the proposed control models:

1. Existing demand scenario: this scenario corresponds to the existing traffic condition for the morning peak period; demands are obtained from the calibrated simulation model directly (Chu, et al 2004);
2. Medium demand scenario: demands are equivalent to 75% of the existing demand scenario;
3. Low demand scenario: demands are equivalent to 50% of the existing demand scenario.

Simulations are performed for a 4½-hour period for each scenario under the baseline control and the adaptive control, respectively. The baseline control corresponds to the free-mode actuated intersection control and the traffic-responsive ramp metering control in the existing network. The first 30 minutes are considered as the warm-up period for vehicles to fill in the network, and only

the last four hours of simulation are analyzed. Five simulation runs are conducted per scenario in order to generate statistically meaningful results. The mean value of simulation results are used for analysis.

7.2 Evaluation of intersection control model

In the adaptive intersection control model, the maximum allowable cycle length, C_{max}, is set equal to 100 seconds for each signal. The total lost time, *L*, is 4 seconds for each actuated phase. The saturation flow rate, *S*, is equal to 1900 veh/hr/lane for each through movement phase, and 1800 veh/hr/lane for each left-turn movement phase. And, to avoid some potential problems in the simulation network, those optimized control parameters that can take on unreasonably small values are further adjusted based on the following rules:

1. If the minimum green time is extremely short (e.g., < 4 sec), it is set to be 4 seconds.
2. If the maximum green time is shorter than the minimum green time, it is set equal to the minimum green.
3. If the unit extension is not greater than *1/S*, which may cause "early gap-out" right after the minimum green, it is set equal to *1/S + 0.1* seconds.

Two groups of performance measures are used for the model evaluation:

1. For isolated intersections: Vehicle Spillover (VSO), Maximum Queue Length (MQL) and Vehicle Travel Delay (VTD).
2. Overall system performance: Average Travel Time (ATT), Average Vehicle Speed (AVS), Vehicle Mileage Traveled (VMT) and Vehicle Hours Traveled (VHT).

As an example, a T-intersection is selected to show the performance of the proposed control model at individual intersections. This intersection corresponds to the junction of Irvine Center Drive and the off ramp from Southbound I-405, as shown in Figure 20. Phases *2* and *6* are assigned to the through movements and operated as min-recall phases, while phase *4* is assigned to the left-turn movement with no recall function. The extension detectors (6'×6') for through phases are placed 300 ft upstream from the stop line, and the call and extension detectors (5'×50') for left-turn phase are placed right behind the stop line. The baseline control parameters for this signal are shown in table 1.

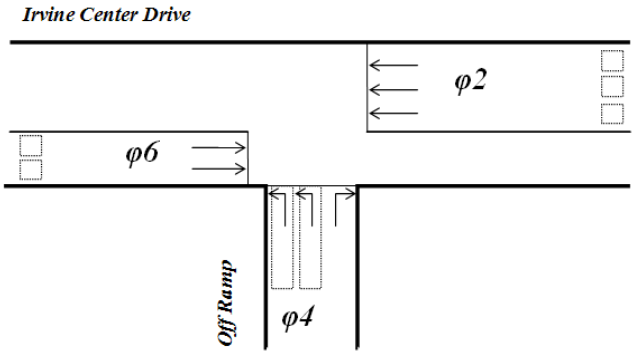

Figure 20. Study Intersection

Table 1. Parameters for the Study Intersection

Phase	2	4	6
Min Green (sec)	8	5	8
Max Green (sec)	40	24	40
Unit Extension (sec)	5.0	2.0	5.0
Yellow and Red (sec)	4.0	4.0	4.0

Here, we present only the simulation results from scenario 1 to demonstrate the impact of the proposed control model at this T-intersection. Figure 21 shows the arrival flow profiles for the three phases during the simulation period. Phases *2* and *4* experience two "peak" periods—around 8am and 9am, respectively—and phase *6* experiences a relatively steady and low level of flow. The profiles under both baseline and adaptive control for each signal phase are very similar due to the use of the same demands for simulation.

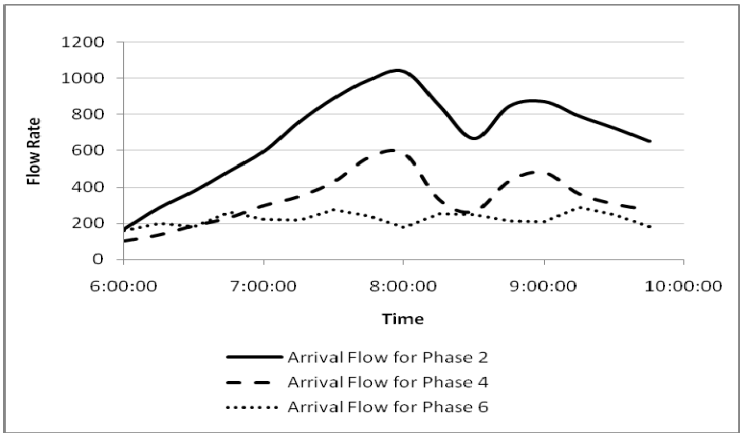

Figure 21. Flow Profile for Each Phase

Table 2 lists the performance measurements resulting from the simulation results for each phase. It can be seen that the vehicle spillover in phase *2* has been decreased by 9, and in phase *4* has been decreased by 8. A possible reason is phase *6* has relatively low flow rate and thus no spillover occurs in this phase. Some reduction in maximum queue length has been achieved with the biggest improvement being 23.5 feet in phase *2*. No improvement has been gained in the maximum queue length for phase *4*, but the travel time for this phase has been reduced by 128.8 vehicle seconds. The travel time is also reduced for phases *2* and *6*. The overall results show some improvement for the entire intersection in each measure of performance.

Table 2. Performance of the Intersection Control

	VSO (number)	MQL (feet)	VTD (second)
Phase 2			
Baseline	29	77.1	683.4
Adaptive	20	53.6	599.3
Improvement	9	23.5	84.1
Phase 4			
Baseline	19	60.1	378.4
Adaptive	11	60.1	249.6
Improvement	8	0	128.8
Phase 6			
Baseline	0	23.0	379.9
Adaptive	0	19.7	362.2
Improvement	0	3.3	17.77
Overall			
Baseline	48	160.2	1441.7
Adaptive	31	133.4	1211.1
Improvement	17	26.8	230.6

The performance of the entire network for all three scenarios is shown in Table 3. It is found that the network under adaptive control performs better than the baseline free-mode actuated control—drivers spend less time in the network and travel more distance with improved traveling speed. It is also found that the performance in scenario 1 is better than that in the other two scenarios, and scenario 3 has gained the least improvement. One possible reason underlying this result is that the extremely low-level traffic flow may behave freely in the network without being affected by the change of control strategies. On the other hand, it can be concluded that, although the vehicle arrival pattern is assumed to be a Poisson process in the model formulation, the performance of the signalized network can also be improved by the proposed adaptive control.

Table 3. Performance of the Network Control

	ATT (second)	AVS (mile/hr)	VMT (mile)	VHT (hour)
Scenario 1				
Baseline	344.3	43.9	760920.0	17367.6
Adaptive	331.0	45.9	762491.2	16725.5
Improvement (%)	3.86	4.56	0.21	3.70
Scenario 2				
Baseline	257.0	59.1	575585.6	9788.2
Adaptive	255.2	59.5	576046.1	9671.8
Improvement (%)	0.86	0.68	0.08	1.19
Scenario 3				
Baseline	249.5	60.9	382327.4	6284.3
Adaptive	248.4	61.1	382649.9	6263.4
Improvement (%)	0.48	0.33	0.01	0.33

7.3 Evaluation of ramp control model

In the adaptive ramp control model, the maximum allowable metering rate, r_{max}, is set equal to 900 veh/hr/lane (i.e., 15 veh/min/lane), and minimum allowable metering rate, r_{min}, is set equal to 240 veh/hr/lane (i.e., 4 veh/min/lane). And, the queue/merge overide operation applies as needed. Two groups of measure of performance are used for the model evaluation:

1. For isolated ramps: Ramp Vehicle Travel Delay (RVTD), (Freeway) Mainline Vehicle Travel Delay (MVTD), and Total Vehicle Travel Delay (TVTD). Note that only the freeway section into which the ramp merges is considered here.
2. Overall system performance: ATT, AVS, VMT and VHT.

As an example, the ramp that corresponds to the onramp from Southbound Jeffery Road to Northbound I-405 (Figure 22) is selected to demonstrate the performance of the proposed control model at individual ramps. The onramp has two vehicle travel lanes merging into one that connects to the four-lane mainline section. The system detectors downstream of the ramp are placed to collect those data (e.g., occupancy and flow) that can be used as input to the ramp control model.

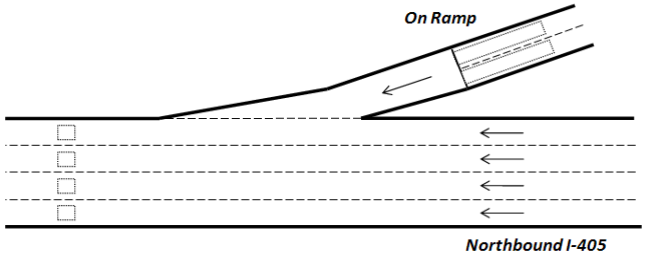

Figure 22. Study Onramp

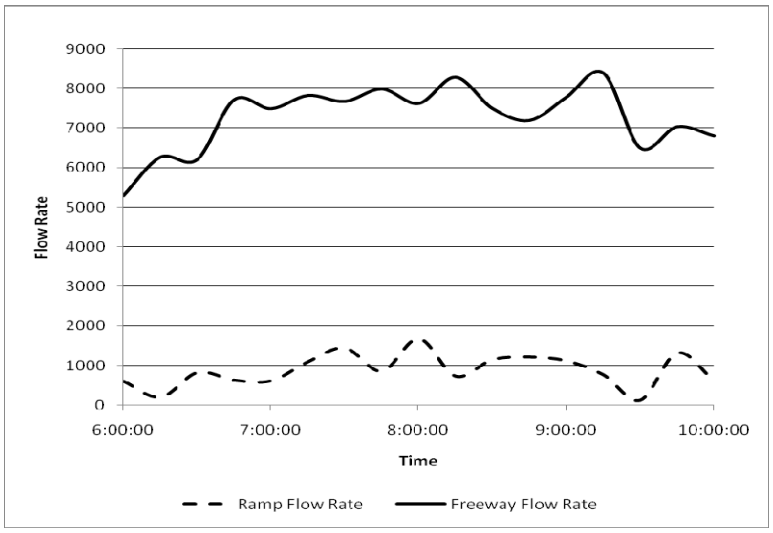

Figure 23. Flow Profile for Onramp and Freeway Section

Figure 23 shows the flow profile for scenario 1 under both baseline and adaptive control for the onramp and freeway, respectively. The profiles are plotted with smoothed lines based on the flow data measured at 15-minute intervals.

Table 4 lists the simulation results with the delay measurements. It can be seen that the vehicle travel delay on ramp is reduced by 976.0 seconds, which means about 70% improvement has been achieved for the ramp. The vehicle travel delay on freeway mainline is also reduced by 52.5 seconds and totally, the vehicle travel delay has been reduced by 1028.5 seconds.

Table 4. Performance of the Ramp and Mainline Sections

	RVTD (second)	MVTD (second)	TVTD (second)
Baseline	1392.3	645.7	2038.0
Adaptive	416.3	593.2	1009.5
Improvement	976.0	52.5	1028.5
Improvement (%)	70.1	8.1	50.0

The performance measures for the entire network for each of the three scenarios are shown in Table 5. It is found that the network under adaptive control performs better than the baseline traffic responsive metering control—drivers spend less time in the network and travel greater distance with improved traveling speed. Similar to the intersection results, the performance in scenario 1 is better than that in the other two scenarios, and scenario 3 has gained the least improvement.

.

Table 5. Performance of the Network

	ATT (second)	AVS (mile/hr)	VMT (mile)	VHT (hour)
Scenario 1				
Baseline	344.3	43.9	760920.0	17367.6
Adaptive	311.2	48.7	765988.7	15745.9
Improvement (%)	9.61	10.93	0.67	9.34
Scenario 2				
Baseline	257.0	59.1	575585.6	9788.2
Adaptive	256.1	59.3	577270.3	9731.4
Improvement (%)	0.35	0.34	0.29	0.58
Scenario 3				
Baseline	249.5	60.9	382327.4	6284.3
Adaptive	248.8	61.1	382900.2	6255.1
Improvement (%)	0.28	0.33	0.15	0.46

7.4 Evaluation of combined intersection/ramp control model

Here, the combined intersection/ramp control is evaluated using the overall system performance measures, ATT, AVS, VMT and VHT. Table 6 lists the simulation results for each of the three scenarios. Again, the network under adaptive intersection control and ramp control performs better than the baseline actuated intersection control and traffic-responsive metering control—drivers spend less time in the network and travel more distance with improved traveling speed. And, the performance in scenario 1 is better than that in the other two scenarios, and scenario 3 has gained the least improvement.

Table 6. Performance of the Network

	ATT (second)	AVS (mile/hr)	VMT (mile)	VHT (hour)
Scenario 1				
Baseline	344.3	43.9	760920.0	17367.6
Adaptive	305.5	49.6	766071.2	15442.5
Improvement (%)	11.27	12.98	0.68	11.08
Scenario 2				
Baseline	257.0	59.1	575585.6	9788.2
Adaptive	255.5	59.4	577585.6	9653.9
Improvement (%)	0.58	0.51	0.35	1.37
Scenario 3				
Baseline	249.5	60.9	382327.4	6284.3
Adaptive	248.3	61.2	383196.6	6252.1
Improvement (%)	0.48	0.49	0.23	0.51

Figure 24 compares the three control models using overall system performance measures. It is found that the combined intersection/ramp control model performs the best in terms of ATT, AVS, VMT, and VHT. The improvement on VMT is very minor since the simulation period for each scenario starts from a free flow condition and ends with another free flow condition.

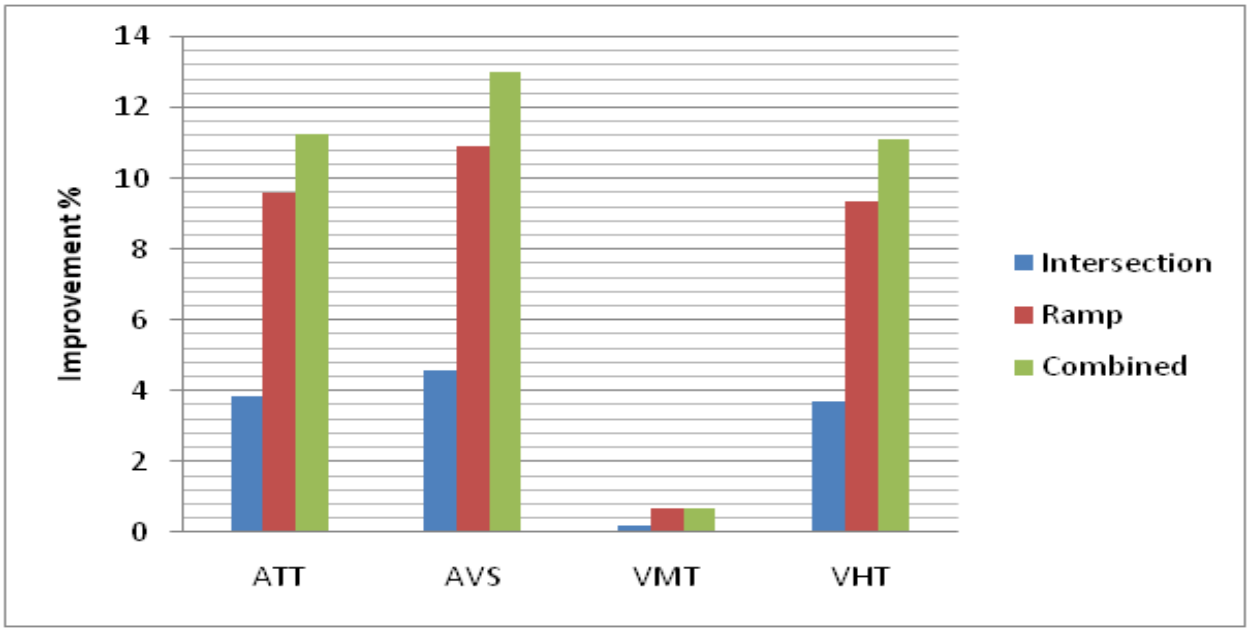

Figure 24. Overall System Performance Comparison of the Three Control Models

8. Concluding Remarks

This project introduces three real-time adaptive control strategies, including an intersection control, ramp control and an integrated control that combines both intersection and ramp control. The development of these strategies is based on a mathematical representation that describes the behavior of real-life processes (traffic flow in corridor networks and actuated controller operation). Only those parameters commonly found in modern actuated controllers (e.g., Type 170 and 2070 controllers) are considered in the formulation of the optimal control problem. As a result, the proposed strategies could be easily implemented with minimal adaptation of existing field devices and the software that controls their operation.

Microscopic simulation was employed to test and evaluate the performance of the proposed strategies in a calibrated network. Simulation results indicate that the proposed strategies are able to increase overall system performance and also the local performance on ramps and intersections. Prior to testing the complete model, separate tests were conducted to evaluate the intersection control model on: 1) an isolated intersection, and 2) a network of intersections along an arterial. The complete model was then tested and evaluated on the Alton Parkway/I-405 corridor network in Irvine, California.

In testing the optimal control model, we simulated a variety of conditions on the freeway and arterial subsystems that cover the range of demand from peak to non-peak, incident to non-incident, conditions. The results of these experiments were evaluated against full-actuated operation and found to offer improved performance.

The scope of the current effort includes the development of the corridor adaptive control model and its testing and evaluation only in a simulation environment. Although actual deployment is beyond the scope of the current effort, we believe that the results of the evaluation of the simulated network warrant further investigation of incorporation of the adaptive control system as a service within the planned CARTESIUS deployment under CTNet (in separate, complementary PATH/Caltrans projects).

Such research deployment could relatively easily be conducted on the Alton Parkway/I-405 corridor network for which we have at least limited authority to conduct tests involving closed-loop control. On the arterial, we have installed a system of Type 2070 controllers at all signalized intersections that operate independently from the local City of Irvine system. We have established real-time communication with these control devices and also receive real-time raw data streams from loop detectors within the study area. In addition, software has been developed, and laboratory tested, that permits real-time adaptive control of the Caltrans District 12 ramp meters in this corridor.

Future efforts will be made to improve this model by: (1) seeking a more sophisticated algorithm that models the actual traffic flow pattern in signalized network; (2) further developing this model in order for the application in coordinated control systems; (3) comparing this model with other adaptive control strategies; and (4) incorporating access/egress choice model in the integrated corridor control.

References

Cameron, Gordon D. B. and Duncan, Gordon I. D. (1996). PARAMICS-Parallel Microscopic Simulation of Road Traffic. The Journal of Supercomputing, Vol.10, No.1, 25-53.

Chang, G-L., Wu, J., and Lieu, H. (1994) Real-time incident-responsive corridor control: a successive linear programming approach. Proceedings of the 4th Annual Meeting of IVHS America, Atlanta, GA, Vol. 2, pp. 907-918.

Chu, L., Liu X., Recker, W. (2004) Using Microscopic Simulation to Evaluate Potential Intelligent Transportation System Strategies under Nonrecurrent Congestion, Transportation Research Record 1886, Transportation Research Board, National Research Council, Washington, D.C., pp.76-84.

Cox, D. R., and Smith, W. L. (1961) *Queues*, London: Methuen.

D'Ans, G. C., and Gazis, D. C. (1976) Optimal Control of Oversaturated Store-and Forward Transportation Networks. *Transportation Science*, Vol. 10, pp. 1-19.

Darroch, J. N. (1964) On the Traffic Light Queue, *Annals Math Statistics*, 35, pp.380-388.

Head, K. L. (1995), "An Event-Based Short-Term Traffic Flow Prediction Model", *Transportation Research Record 1510*, pp. 45-52.

Hokstad, P. (1979). A single-server queue with constant service time and restricted accessibility. *Management Science*. 25, 2, pp. 205-208.

Kleinrock, L. (1975). *Queueing Systems. Volume 1*. Wiley. New York.

Lowrie, P.R. (1992) "SCATS: A Traffic Responsive Method of Controlling Urban Traffic Control", *Roads and Traffic Authority*.

Papageorgiou, M. (1995) An Integrated Control Approach for Traffic Corridors. *Transportation Research-C*3, No. 1, pp. 19-30.

Robertson, D.I. and Bretherton, R.D. (1991) "Optimizing Networks of Traffic Signals in Real Time – the SCOOT Method", *IEEE Transaction on Vehicular Technology*, Vol. 34, pp. 11-15.

Sims, A.G., (1979), "The Sydney Coordinated Adaptive Traffic System.", *Proceedings of the Engineering Foundation Conference on Research Priories in Computer Control of Urban Traffic Systems*, pp. 12-27.

Singh, M. G. and Tamura, H. (1974) Modelling and hierarchical optimization for oversaturated urban road traffic networks. *International Journal of Control*, Vol. 20, No. 6, pp. 913-934.

Stephanedes, Y. J., and Chang, K-K. (1993) Optimal Control of Freeway Corridors. *Journal of Transportation Engineering*, Vol. 119, No. 4, pp. 504-514.

Takacs, L. (1955). Investigation of waiting time problems by reduction to Markov processes. *Acta Math. Acad. Sci. Hungary*. 6, pp 101-129.

Ziliaskopoulos, A. K. (2000) A linear programming model for the single destination system optimum dynamic traffic assignment problem. *Transportation Science*, Vol. 34, No. 1, pp. 37-49.